D.S.S. CONTRACT OST85-00428

DETERMINATION OF STRESS INTENSITY FACTORS FOR WELD TOE DEFECTS

Phase III Report

March 1988

Prepared by:

R. Bell P.Eng.

FACULTY OF ENGINEERING

CARLETON UNIVERSITY

DETERMINATION OF STRESS INTENSITY FACTORS FOR WELD TOE DEFECTS PHASE III

FINAL REPORT

BY

R. BELL, P.Eng.

Work on this project was conducted under the auspices of Physical Metallurgy Research Laboratories Canada Centre for Mineral and Energy Technology, Energy, Mines and Resources Canada.

DSS FILE NUMBER: 20ST.23440-6-9008

DSS CONTRACT SERIAL NUMBER: OST85-00428

CANMET PROJECT NUMBER:

CANMET SCIENTIFIC AUTHORITY: Dr. O. Vosikovsky

85 pp

March 1988

This report should be cited by D.S.S. File No. 20ST.23440-6-9088/1

MICROMEDIA

ABSTRACT

This report describes the work carried out to fulfill the requirements described by the work statement of D.S.S. Contract Number OST85-00428, a copy of which is included as Appendix I.

A fatigue life prediction program, based on Linear Elastic Fracture Mechanics (LEFM), has been developed. The results of this prediction model has been validated by comparison with test results for welded "T" plate joints.

This life prediction program has been extended to include the capability of variable amplitude loads.

Finite element investigations have been carried out to determine the stress distribution near the weld toe of welded "T" plate joints.

Preliminary work has been carried out to develop a procedure to obtain the SIF's at the weld toe of a Pipe-to-Plate joint using the finite element method.

The contractor has attended several ECSC-Canada progress meetings as required by the contract.

RESUME

Ce raport décrit le travail effectué pour compléter les conditions requises par le contrat du M.A.S. numéro OST85-00428, dont une copie est incluse en Appendice 1.

Le programme de prédiction de la durée de vie, basé sur la mécanique linéaire élastique de la rupture, a été developpé. Les résultats de ce modèle de prédiction ont été comparés aux résultats de tests des soudures de tôles en "T".

Ce programme de prédiction de la durée de vie a été étendu pour inclure les charges d'amplitude variable.

Des calculs par éléments finis ont été exécutés pour déterminer la distribution des contraintes près du cordon des soudures en "T".

Le travail préliminaire a été exécuté pour développer une procédure de calcul des facteurs d'intensité des contraints au pied de soudures de tubes sur des tôles par une analyse aux éléments finis.

L'entrepreneur a assisté à plusieurs conférences de CECA-Canada tel que requis par le contract.

TABLE OF CONTENTS

		Page
	ABSTRACT	2
1.	**INTRODUCTION**	6
1.1	Conclusions of Phase I Report	6
1.2	Conclusions of Phase II Report	8
1.3	Contents of Phase III Interim Report	8
2.	**FATIGUE LIFE PREDICTION**	11
2.1	Fatigue Life Prediction Program	11
2.2	Modifications to Life Prediction Programs	13
2.3	Fatigue Life Predictions	15
2.4	Fatigue Crack Growth Thresholds	16
3.	**VARIABLE AMPLITUDE LOADING**	31
3.1	Introduction	31
3.2	Modifications to Life prediction Program	31
3.3	Variable Amplitude Loading	31
3.4	Common Load Sequence	33
3.5	Cumulative Damage	34
3.6	Variable Amplitude Results	35
4.	**DISTRIBUTION OF STRESS NEAR THE WELD TOE**	42
4.1	Introduction	42
4.2	Stress Concentration Factors	42
4.3	Correlation of SCF's with Empirical Relations	43
4.4	Fatigue Notch Factor	43
4.5	Stress Distribution Near the Weld Toe	45
5.	**ANALYSIS OF PIPE-TO-PLATE JOINTS**	58
5.1	Introduction	58
5.2	Pipe-to-Plate Joint	58
5.3	Methodology for Finite Element Analysis	58
6.	**REPORT ON ECSC-CANADA MEETINGS**	65
6.1	ECSC Progress Meeting, Copenhagen.	65
6.2	Canada-ECSC Progress Meeting, Halifax.	65
6.3	Contract Progress Meetings.	65
6.4	Conference at Delft in June 1987.	66
7.	**CONCLUSIONS**	67
8.	**REFERENCES**	68

APPENDIX I

APPENDIX II

APPENDIX III

ACKNOWLEDGEMENT

This work was performed for the Physical Metallurgy Research Laboratories, CANMET, the Department of Energy, Mines and Resources Canada under Supply and Services Canada Contract OST85-00428. The author is indebted to PMRL CANMET for permission to publish this work. The author also acknowledges the support and contribution received from Dr. O. Vosikovsky, PMRL in the Scientific administration of the contract.

DISCLAIMER

Any data presented, opinions, findings, conclusions, or recommendations expressed in this report are those of the author and do not necessarily reflect the views of CANMET. Crown copyright of this report is reserved.

1. INTRODUCTION.

This report is the final report on the D.S.S. Contract OST85-00428. This is Phase III on the project entitled "Determination of Stress Intensity Factors for Weld Toe Defects". The work statement of this phase of the contract is given as Appendix I.

Phase I of the project reviewed the literature regarding the application of fracture mechanics to the prediction of fatigue crack growth of weld toe defects at tubular joints of offshore structures. Also included was a discussion on the use of the finite element method for the determination of fracture parameters and the numerical calculation of stress intensity factors, (SIF).

During this phase of the project the general purpose finite element program ASAS was used to model a welded "T" plate specimen, Figure 1.1, with a weld toe defect. Two and three dimensional analyses were performed and the SIF for a range of defects were obtained [1].

In the 2-dimensional case stress intensity factors were presented for a series of straight fronted cracks with crack-thickness ratios, a/t, ranging from 0.005 to 0.7 for three different weld profiles. Empirical expressions were obtained from these results to describe the variation of the SIF as function of a/t.

In the 3-dimensional studies crack tip stress intensity factors were obtained for semi-circular and semi-elliptical weld toe cracks. The crack geometries investigated had aspect ratios, c/a, of 1.0, 0.5 and 0.25 and depth-thickness ratios, a/t, in the range 0.05 to 0.4 and the weld had profiles of 30^{0}, 45^{0} and 70^{0}.

Phase II of the contract described further 3-dimensional finite element studies carried out to supplement the Phase I data for the SIF of elliptical weld toe cracks in welded "T" plate joints. Curves were fitted to this stress intensity factor data and a computer program was written to predict the fatigue crack growth and the life of welded joints. The validity of this prediction program was assessed by comparison of predicted results with experimental data obtained in the Canadian offshore steels research program.

For convenient reference the conclusions of Phase I and II of the contract are summarized below, [1] - [2].

1.2 Conclusions of Phase I Report.

1. The work described in this report utilizes the finite element program ASAS together with a specially developed mesh generator to efficiently analyze the welded "T" specimens using linear elastic fracture mechanics.

2. The requirements of the original and amended work statements have been met giving FEM results for 2-dimensional and 3-dimensional determination of the SIF at weld toe cracks.

3. Results using 2-dimensional finite element analyses are presented for a range of weld toe cracks with crack depths between a/t = 0.005 and 0.7 and weld profiles of 30^{o}, 45^{o} and 70^{o}.

4. Empirical equations are fitted to the above 2-dimensional SIF results. These equations agree well with the FEM results for the weld angles considered to with 2 to 3 percent, depending on the crack depth.

5. A stress analysis was performed on a series of uncracked "T" joints to obtain the stress distribution and the stress concentration factor, SCF, at the weld toe region. It was found from these analyses for the 3-point bending loadcase that the distance of the support points from the weld toe has an effect on the SCF. For the cases considered this effect is quite small,(5 - 13%); however further analyses should be performed to obtain the variation of SCF for a series of geometrically similar joints as the support distance is reduced.

6. Accuracy studies were performed on a semi-elliptical surface crack in a cube subjected to tension. These analysis indicated that, for the best compromise between accuracy and computing cost, the mesh in the region of the crack should be constructed with a minimum of four crack tip elements around the crack, and the dimensions of these elements should be approximately m/L = 2 and a/L = 5.

7. The SIF for a series of crack shapes and crack depths for three different weld profiles are presented. In the main these results are for crack depths less than a/t = 0.1, which is the region indicated by the 2-dimensional studies where the weld profile has the greatest effect on the SIF obtained.

8. The variation of SIF around semi-circular and semi-elliptical crack shapes of a/c = 1.0, 0.5 and 0.25 and crack depths, a/t varying between 0.025 and 0.4 are presented. The effect of crack shape, crack depth and weld angle on the SIF is demonstrated.

9. The versatility of the ASAS substructuring capability has been demonstrated in these studies. This program facility together with the aforementioned mesh generator for elliptical crack FEM meshes permitted the 3-dimensional studies to be carried out a reasonable cost.

1.2 Conclusions of Phase II Report.

1. The requirements of the Phase II work statement have been met.

2. The general purpose finite element program ASAS has been used to expand the data base od 3-D finite element results for the SIF at weld toe defects with varying c/a and a/t ratios.

3. A computer program was written to predict the fatigue life of welded "T" plate joints. This program has the capabilities described in section 3.2 of this report.

4. The life prediction program has a prescribed crack shape development capability so that multiple crack growth and coalescence can be simulated.

5. An investigation was carried out to study the effect of initial crack size on the predicted life of welded "T" plate specimens. These results are presented in tabular and S-N diagram form.

6. The predicted fatigue life of the "T" plate specimens compared favourably with the published experimental results.

7. A 2-dimensional finite element study was performed to investigate the effect of support span on the SIF's obtained.

8. It was found that for the geometries and loading spans considered in this work no correction to the SIF values need be applied.

1.3 Final Report on Phase III of the Contract.

The following report describes the work carried out in Phase III of the contract.

Chapter 2 describes modifications to the fatigue crack growth prediction program and compares the prediction results by comparison with experimental test results for welded "T" plate joints produced in the Canadian offshore steels research program. These results are being published in the conference "Steels in Marine Structures", in Delft, The Netherlands (June 1987). A copy of this paper is included as Appendix II.

In chapter 3 the implementation of a Variable amplitude loading capability in the fatigue life prediction program is described. The European COLOS (Common Load Sequence) data is included to produce a realistic load history. The Miner summation procedure for calculating cummulative damage was also included in the program.

Chapter 4 presents a 2-dimensional finite element analysis to determine the stress distribution near the weld toe of "T" plates for a range of thicknesses and weld toe radii ranging from 0.2 to 10 mm.

Chapter 5 describes the work performed in developing a procedure for obtaining SIF's at the weld toe of pipe-to-plate joint using 3-D finite element methods.

Chapter 6 details the attendance of the principal investigator at Canada-ECSC progress meetings as required by the contract.

Chapter 7 gives conclusions of this phase of the work and indicates areas where further work would enhance the fatigue life prediction capabilities of the Canadian Offshore Research Program.

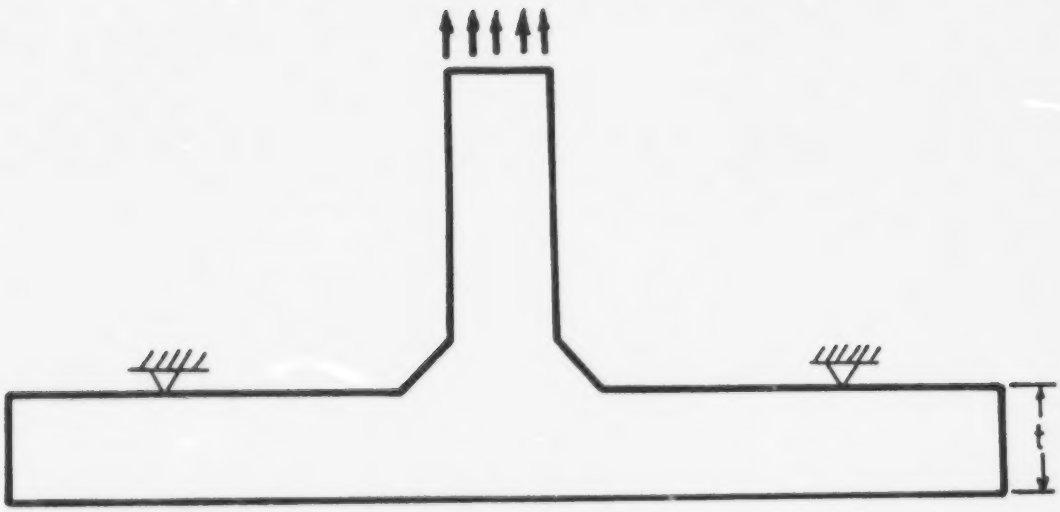

"T" SPECIMEN

FIG. 1·1

2. FATIGUE LIFE PREDICTION.

2.1 Fatigue Life Prediction Program

A fatigue life prediction program was developed based on linear elastic fracture mechanics, (LEFM). In this case the fatigue crack growth can be described by a single parameter, the stress intensity factor, K. Also the crack growth rate can be related to the variation in stress intensity factor ΔK by a growth law such as the Paris Law.

$$da/dN = C\,\Delta K^m \tag{2.1}$$

where C and m are material constants and ΔK is given by

$$\Delta K = Y\,\Delta\sigma\,\sqrt{\pi a} \tag{2.2}$$

and Y is a factor describing the geometry of the component and the crack. The stress intensity factor describes the stress environment at the crack tip and for two different geometries of the same material the stress distribution will be identical if the stress intensities are equal. It follows that the fatigue crack propagation in the two bodies will be the same if the cyclic variation in ΔK is the same.

The life of a component can be predicted by integration of equation (2.1) as:

$$N = \frac{1}{C}\int_{a_i}^{a_f} \frac{da}{(\Delta K^m)} \tag{2.3}$$

Thus the number of cycles N, to propagate a crack from an initial size a_i to a final size a_f, can be calculated.

The fatigue life prediction program developed in this work is described in detail in [2] but for convenience the capabilities, inputs and output of the program will be summarized below.

The program has the following capabilities:

1. **GROWTH LAWS**

   The growth of a fatigue crack can be modelled according to the following growth laws:

   (i) Paris Law [3]
   (ii) Forman Law [4]
   (iii) Collipriest Law [5]
   (iv) Paris Law with Two Regions
   (v) Klesnil and Lukas Law [6]
   (iv) Schulz Law [7]

2. STRESS INTENSITY FACTOR EVALUATION

The stress intensity factor can be evaluated according to the following relationships:

A STRAIGHT FRONTED CRACKS

(i) Gurney and Johnston Equation [8]
(ii) Bell and Kirkhope Equation [28]

B SEMI-ELLIPTICAL SURFACE CRACKS

(i) Newman and Raju Equation [9]
(ii) Bell S.I.F. data [28]
(iii) Irwin Equation [10]

3. LOADING CONDITIONS

The following loading conditions can be simulated:

(i) Constant Amplitude Loading
(ii) Variable Amplitude Loading - block method
(iii) Variable Amplitude Loading - COLOS sequence

The variable amplitude loading options of the program will be described in chapter 3.

4. INITIAL AND FINAL CONDITIONS

The program permits the following initial parameters to be set:

(i) Initial crack depth and shape
(ii) Final crack depth
(iii) Crack growth cycle increment
(iv) Initiation cycles
(v) Material Constants
(vi) Output Cycle Increment

5. CRACK SHAPE DEVELOPMENT MODELS

The program has the capability to model the following shape development of weld toe crack.

(i) Straight fronted crack (SCF)
(ii) Natural development of a single semi-elliptical crack (SC1)

(iii) Development of a single semi-elliptical crack with a constant a/c value (SC2)

(iv) Coalescence of multiple weld toe cracks and development at a constant a/c value (MC1)

(v) Coalescence of multiple weld toe cracks and development as a straight fronted crack (MC2)

These crack shape development will be described in section 2.2.

6. PROGRAM OUTPUT

The following output information is obtained from the program:

(i) Number of cycles - N
(ii) Crack semi-minor axis length - a
(iii) Crack semi-major axis length - c
(iv) Stress Intensity factor Range - ΔK
(v) Crack Growth Rate - da/dN
(vi) Miner Sum (Variable amplitude loading)

2.2 Modifications to the Life Prediction Program

During this phase of the contract several modifications and enhancements to the program have been made.

The major change to the prediction program is the inclusion of a variable amplitude loading capability and this will be described in detail in section 3.3. Several minor changes have been made in the output of data to make the presentation of information from the various crack geometries and growth laws more consistent.

As stated in section 2.1 several modifications were made to the crack shape development models which are included in the program. The models which are shown diagrammatically in figure 2.8 will be described briefly below.

(i) The SCF model.

The SCF case models the growth of a straight fronted crack using the SIF equations developed by Bell and Kirkhope [1] using 2 dimensional finite elements.

(ii) The SC1 model.

The SC1 case models the 'natural' growth of a single semi-elliptical crack. In this model the crack growth in the a and c directions is calculated independently using the Paris equation using the SIF values at the deepest and surface points of the crack which were obtained using 3 dimensional finite elements [2].

(iii) The SC2 model.

The SC2 model permits the crack to grow as a single semi-elliptical crack but the crack shape is maintained at a constant aspect ratio of a/c = 0.2 throughout the propagation phase.

(iv) The MC1 model.

The MC1 model is a single crack model with a forcing function for a/c to account for multiple initiation and coalescence of cracks along the weld toe. This forcing function is an empirical relationship

$$a/c = e^{-ka} \tag{2.4}$$

which was developed from experimental plate results as described in [13]. When the crack develops to an aspect ratio of a/c = 0.2 the crack shape is maintained constant until the end of the propagation phase of life.

(v) The MC2 model.

The MC2 model is also a single crack model with a forcing function for a/c to account for coalescence of multiple cracks as described in (iv). It also accounts for the crack growing through the edges of the plate. To simulate the crack breaking through the edges the model is modified to the SFC case at a/c = 0.2. At this point the growth calculations are performed using the 2 dimensional SIF relationships.

Other changes which improved the prediction behaviour of the program was the introduction of local smoothing of SIF values as the program switches between semi-elliptical and straight fronted crack growth when using the option of the program which simulates multiple growth and coalescence of weld cracks. This was incorporated in the software because there is a sudden increase in SIF values evaluated by the 3-dimensional semi-elliptical crack solution and the 2-dimensional straight fronted crack solution for the same crack depth.

Several auxiliary programs have also been written to enhance the output and plotting capabilities of the software. A post-processing program was written to take the numerical output of the life prediction program and re-format for a plotting program. The plots shown in Figure 2.2 were produced using this software. Also a program was written which utilizes the stress intensity evaluation routine to produce crack growth rate, da/dN and ΔK data for plotting purposes. This program uses the seven point Incremental Polynomial method for computing da/dN as outlined in ASTM Publication E 647.

The life prediction software described above was also modified to run on the Carleton University CP6 mainframe computer and FPS-64 attached processor. The latter version of the program was developed to make computer predictions using variable amplitude loading more cost effective.

2.3 Fatigue Life Predictions

In order to demonstrate the results obtained from the above prediction program fatigue life predictions for welded "T" plate specimens were compared with experimental data obtained in the Canadian offshore steels research program. These results are also reported in references [12] and [26].

The specimen geometries considered were those described in [11] and shown in Figure 2.1. In the first series of predictions (reference [12]) the specimens were loaded in three point bending, the nominal weld angle was 45^0 and the case of multiple crack initiation and coalescence was simulated. This was carried out by prescribing the crack shape development using an empirical equation derived from the experimental results. This procedure is described in detail in [2] and [12]. The value of initial crack depth was assumed to be 0.5 mm, a value considered to be a valid initial for the application of LEFM and also the smallest crack size that could be repeatably detected with confidence using the crack measuring systems employed in the Canadian experimental program.

In all the predictions the values of C and m were:

$$m = 3.0$$
$$C = 5.36 \times 10^{-12}$$

and the units in equation (2.1) were m/c for da/dN and MPa$\sqrt{m}$ for ΔK. These values were chosen after a study of the literature describing extensive experimental work carried out in Europe on similar steels.

An extensive series of computer runs were performed on five specimen thicknesses at stress levels of 75, 100, 150, 200, and 300 MPa and at a stress ratio of 0.05 to assess the behaviour of the prediction program. These results are presented in detail in reference [12] but for convenience some of this data is reported below.

Figure 2.2 shows a plot of a/N for a "T" plate specimen of thickness, t = 78 mm, loaded in 3-point bending at a stress level of 100 MPa. In this plot be capabilities of the program to prediction the crack growth of a weld toe crack as (i) a straight fronted crack, (SFC case) using the 2-dimensional SIF equations; (ii) a single semi-elliptical crack, (SC1 case), using the SIF data of Bell [2] (iii) a multiple crack case including crack coalescence, (MC2 case). In the latter case the crack grows from an initial crack depth of 0.5 mm changing shape with growth according to the empirical relationship given by equation (2.4) until it is assumed to be a straight fronted crack at a depth of a/c = 0.2. From this point on growth predictions use the 2-dimensional SIF relationships until failure at a depth of a/t = 0.5. Also included in this figure are the experimental data of Vosikovsky et al [13].

Figure 2.3 shows an S-N plot of the complete set of Canadian experimental data compared with the predicted S-N lines for propagation life produced by the life prediction program.

Figures 2.4 - 2.6 show the data of Figure 2.3 presented as life - thickness plots for three stress levels of 100, 150 and 200 MPa. Also included in these plots are data from experimental projects carried out in Europe. In this case total life is plotted and the so called thickness effect can be clearly seen.

Figure 2.7 presents the experimental and predicted data in the form of a log-log plot of relative fatigue strength versus thickness. In this case the data is presented for an endurance life of 1 x 10^6 cycles and normalized for a thickness of 32 mm. Also shown on this plot is the Gurney line of slope -0.25 and experimental data from Europe and Canada.

To further demonstrate the capabilities and accuracy of the life prediction program an extensive series of predictions were carried out for the welded "T" plate joints described above. These results are reported in [26].

Figure 2.8 illustrates the crack shape development models described in section 2.2 together with the experimental crack shape developments made in the Canadian tests [11]. It can be seen that the SC1 or SC2 models do not follow the experimental crack shape development and that in order to model the crack coalescence behaviour of the joints during the first few millimeters of growth the MC1 or MC2 models must be used.

The natural crack growth of a single crack using the SC1 model is shown in Figure 2.9 for a 78 mm "T" plate joint with a hot spot stress of 150 MPa. An initial crack depth of 0.5 mm was chosen and the crack shape development for initial aspect ratios, a/2c, of 0.1, 0.2, 0.3, 0.4 and 0.5 are shown. The numerical propagation lives for these predictions are also given in Table 2.1 and it can be seen that the initial defects develop the same shape and that the initial shape has almost no effect on the predicted propagation life.

In order to compare the predictions obtained using each of the models described in the previous section a series of analyses were performed for a plate thickness of 78 mm and a hot spot stress of 150 MPa. These results are presented in Table 2.2 together with the statistical data from the Canadian experimental program [11].

In general the prediction of the SC1 model are always high, and the MC1 and MC2 model, which account for coalescence give better predictions compared to the experimental data. The SC2 model gives results which lie between the MC1 and MC2 predictions. The MC2 model which accounts for both coalescence and edge cracking gives a remarkably close prediction to the combined data sets.

To illustrate the thickness effect this data is presented in Table 2.3 in which the results are normalized with respect to the 16 mm results in which edge cracking did not occur during the test period. It can be seen that in all cases the models which do not account for edge cracking, (i.e. SC1, SC2 and MC1), underestimate the thickness effect observed in the experiments. The MC2 model predictions which account for both coalescence and edge cracking slightly overestimates the thickness effect in most cases.

2.4 Fatigue Crack Growth Thresholds

In order to investigate the effect of fatigue crack growth thresholds on, (ΔK_{th}), on the fatigue limit a limited series of computer predictions were performed on the "T" plate geometries described in section 2.3. In each case the initial crack depth was 0.5 mm, the initial crack shape was a/c = 0.5 and the crack shape model used was the MC2 model.

For each thickness the stress level was adjusted so that an initial stress intensity range of ΔK = 2, 3 and 4 was obtained. These values of ΔK_{th} were chosen because it was assumed that in the experimental specimens the threshold stress intensity factor will be reduced because these specimens were tested in the "as welded" condition and therefore contain high tensile residual stresses in the weld toe region which would result in a high stress ratio. This high stress ratio causes a lower threshold value of ΔK_{th}.

The results from these predictions are shown in Table 2.4. It can be seen from this table that the fatigue limit at each threshold value is dependent on thickness and reduces with increasing thickness. This phenomenon was also observed in the experimental tests where the fatigue limit, for the range of thicknesses tested, was estimated to vary from 110 MPa for 16 mm plate to 70 MPa for 103 mm plate. It could therefore be concluded that for the specimens tested in the as welded condition the threshold stress intensity factor was in the range 2 - 3 MPa $\sqrt{m}$.

TABLE 2.1

N_p (kcycles) from a_i = 0.5mm to a_f = a/T = 0.5, predicted with model SC1 for natural growth of a single crack ($\Delta\sigma$ = 150 MPa)

Plate Thickness	$a_f/2c$				
	0.1	0.2	0.3	0.4	0.5
16mm	1720	1800	1840	1865	1880
26mm	1420	1480	1505	1515	1530
52mm	1050	1085	1095	1110	1113
78mm	864	888	895	903	905
103mm	725	746	750	755	780

TABLE 2.2

N_p (kcycles) from a_i = 0.5 mm to a_f = a/T = 0.5, ($\Delta\sigma$ = 150 MPa)

Plate Thickness	LEFM Predictions				Statistical Analysis Of Expt. Data	
	SC1	SC2	MC1	MC2	UW	CANMET
16 mm	1880	1080	1680	1397	1732	894
26 mm	1400	890	1170	768	715	558
52 mm	1100	595	620	326	393	249
78 mm	900	435	470	217	408	257
103 mm	750	315	365	170	248*	130*

* brittle fracture at a = 20 mm

SC1 - natural growth of a single crack

SC2 - single crack with fixed aspect ratio (a/2c = 0.1)

MC1 - single crack with forcing function for crack shape to account for coalescence

MC2 - single crack with forcing function for crack shape to account for coalescence and the formation of a an edge crack

TABLE 2.3

Thickness Effect Ratios Based on N_p (kcycles from Table 2.2)

Thickness	LEFM Predictions				Statistical Analysis	
	SC1	SC2	MC1	MC2	UW	CANMET
16/26	1.3	1.2	1.4	1.8	2.4	1.5
16/52	1.7	1.8	2.7	4.3	4.4	3.6
16/78	2.1	2.5	3.6	6.4	4.2	3.5
16/103	2.5	3.4	4.6	8.2	7.0*	6.9*

* brittle fracture at a = 20 mm

SC1 - natural growth of a single crack

SC2 - single crack with fixed aspect ratio (a/2c = 0.1)

MC1 - single crack with forcing function for crack shape to account for coalescence

MC2 - single crack with forcing function for crack shape to account for coalescence and the formation of a an edge crack

TABLE 2.4

Fatigue Limit for Varying Threshold Values

ΔK_{th}	= 2	= 3	= 4
t (mm)	Fatigue Limit (MPa)		
16	82	117	150
26	80	115	145
52	77	111	138
78	75	110	135
103	73	106	132

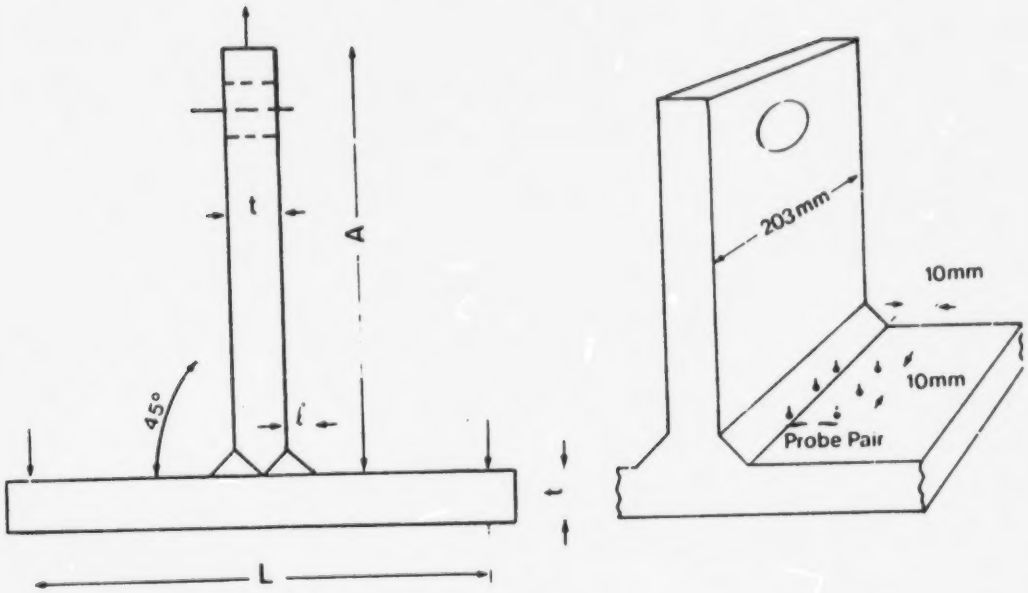

JOINT	t (mm)	ℓ (mm)	L (mm)	A (mm)
A	16	8-12	300	406
B	26	14-18	442	406
C	52	26-30	442	406
D	78	38-42	584	457
E	103	52-56	726	457

FIGURE 2.1

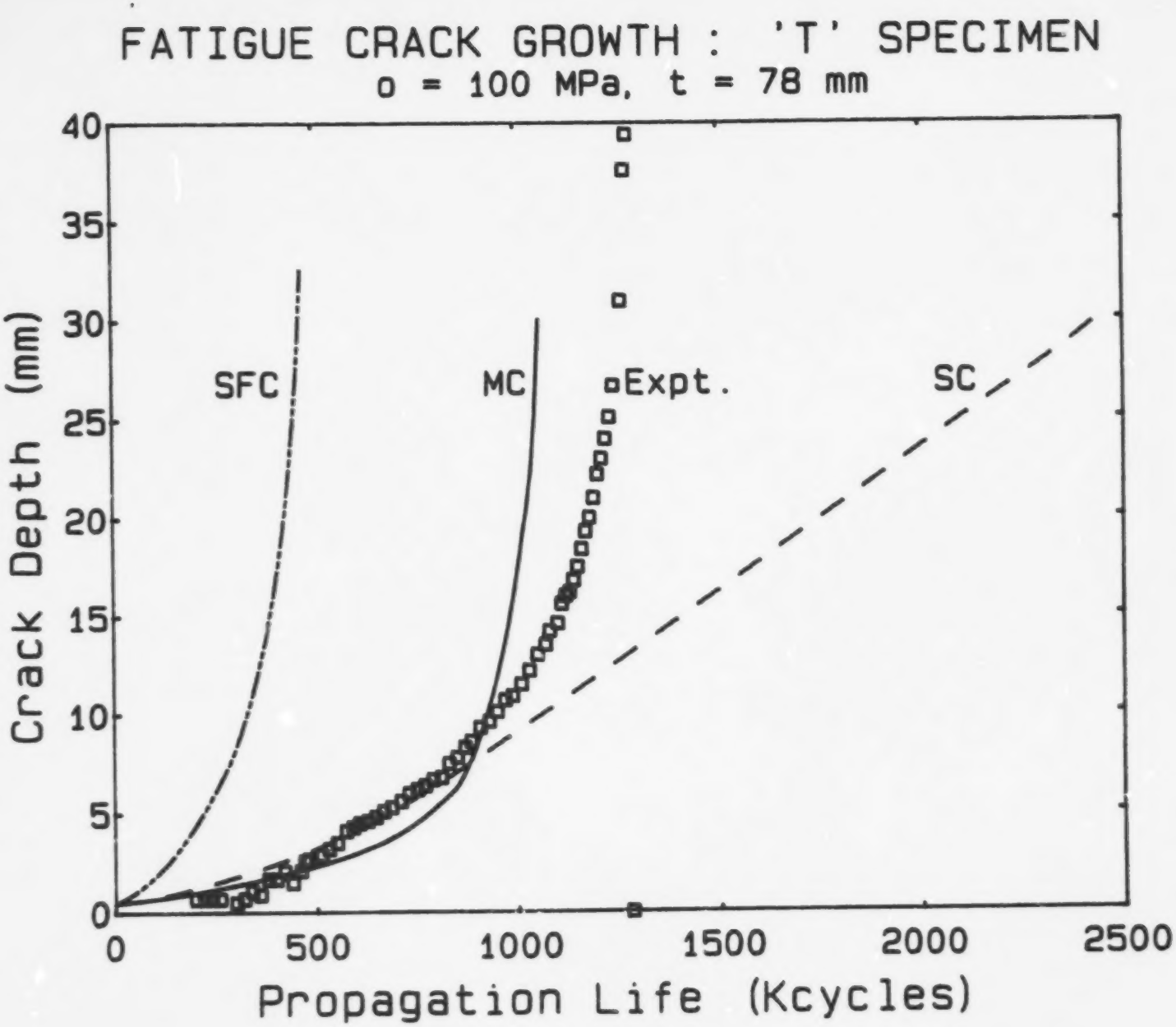
FATIGUE CRACK GROWTH : 'T' SPECIMEN
σ = 100 MPa, t = 78 mm
Crack Depth (mm)
Propagation Life (Kcycles)
SFC
MC
Expt.
SC
0
5
10
15
20
25
30
35
40
0
500
1000
1500
2000
2500

FIGURE 2.2

Predicted Propagation Life Compared
With Canadian Experimental Data

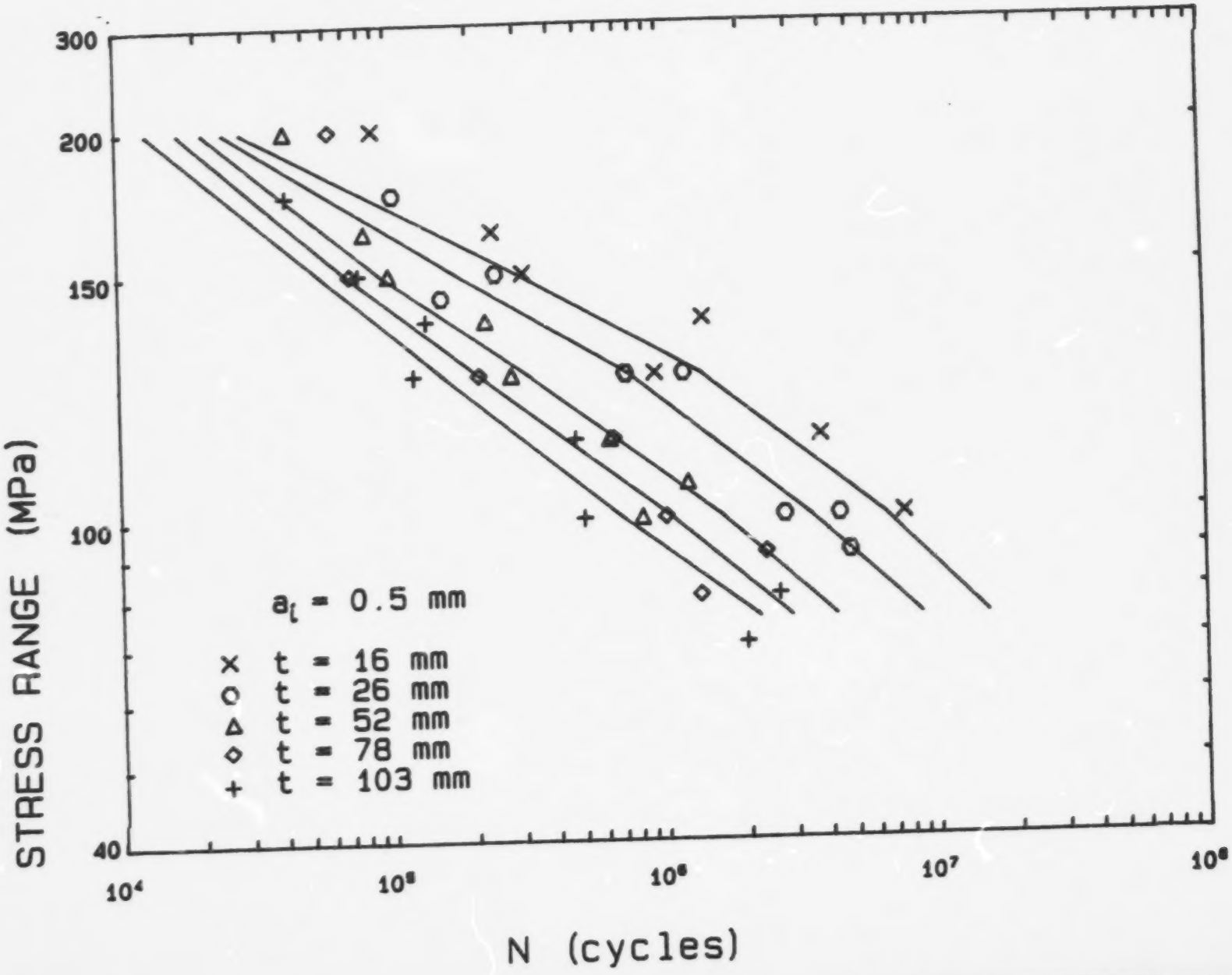

FIGURE 2.3

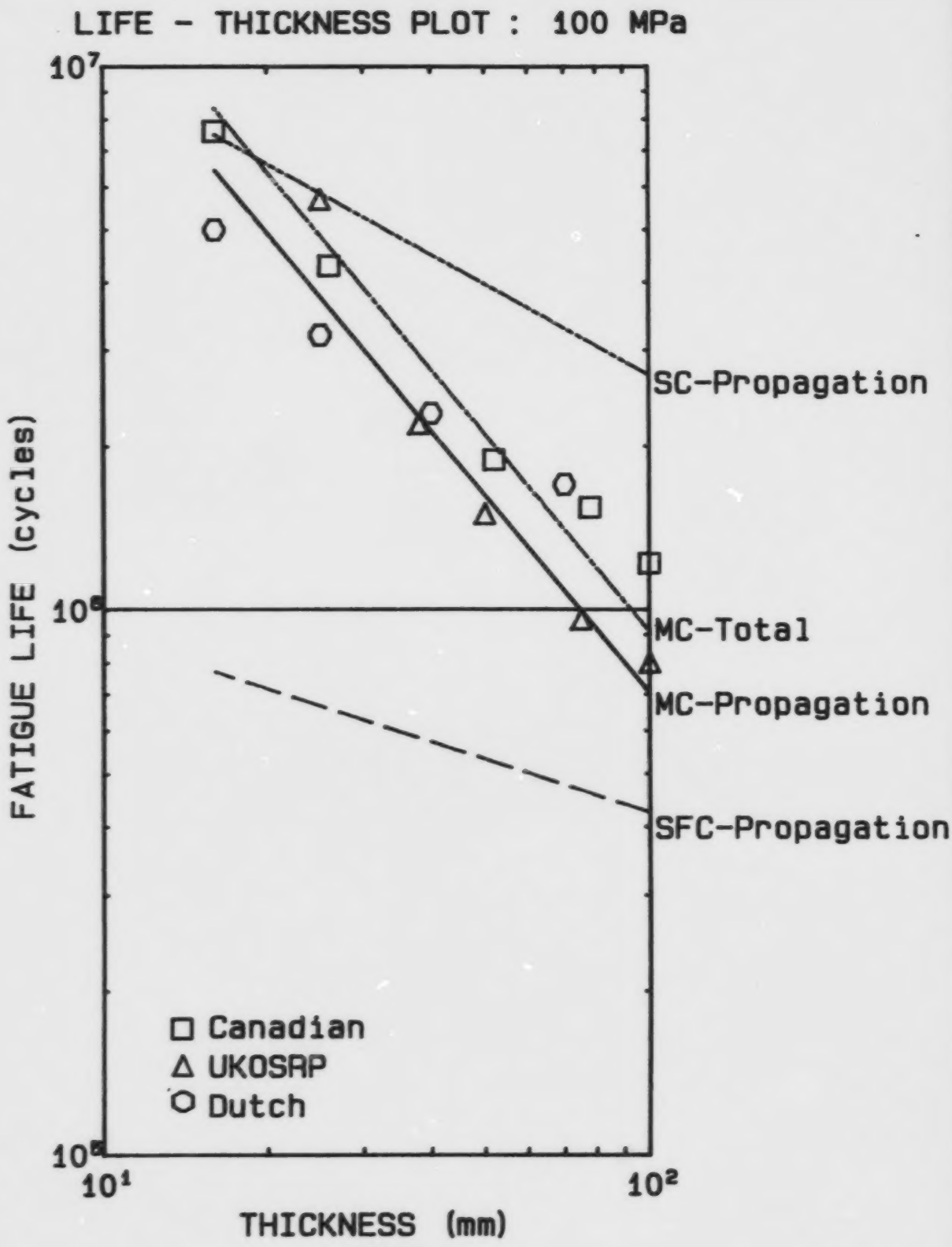
LIFE - THICKNESS PLOT : 100 MPa
10^7
10^6
10^5
10^1
10^2
FATIGUE LIFE (cycles)
THICKNESS (mm)
SC-Propagation
MC-Total
MC-Propagation
SFC-Propagation
Canadian
UKOSRP
Dutch

FIGURE 2.4

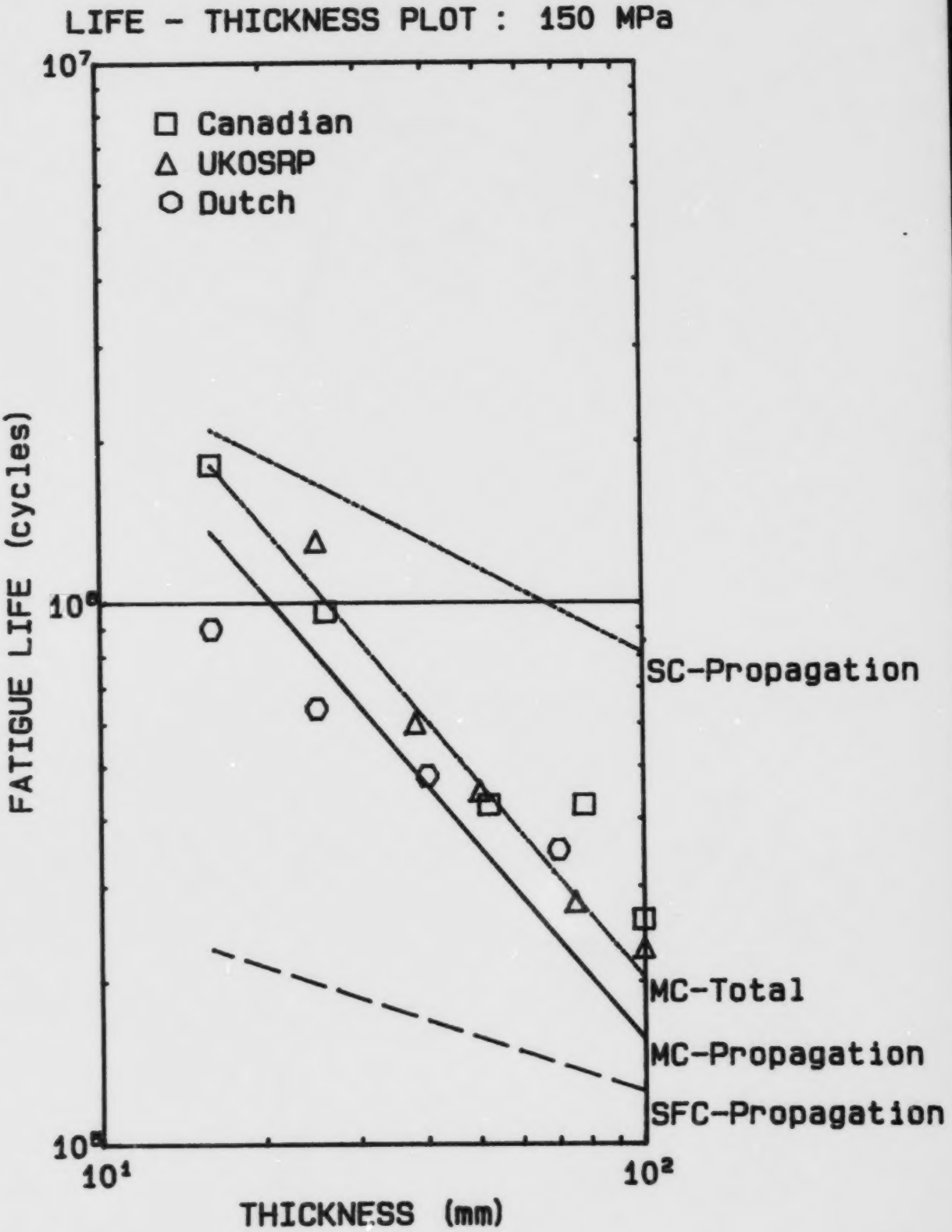
LIFE - THICKNESS PLOT : 150 MPa
Canadian
UKOSRP
Dutch
SC-Propagation
MC-Total
MC-Propagation
SFC-Propagation
FATIGUE LIFE (cycles)
THICKNESS (mm)
10⁷
10⁶
10⁵
10¹
10²

FIGURE 2.5

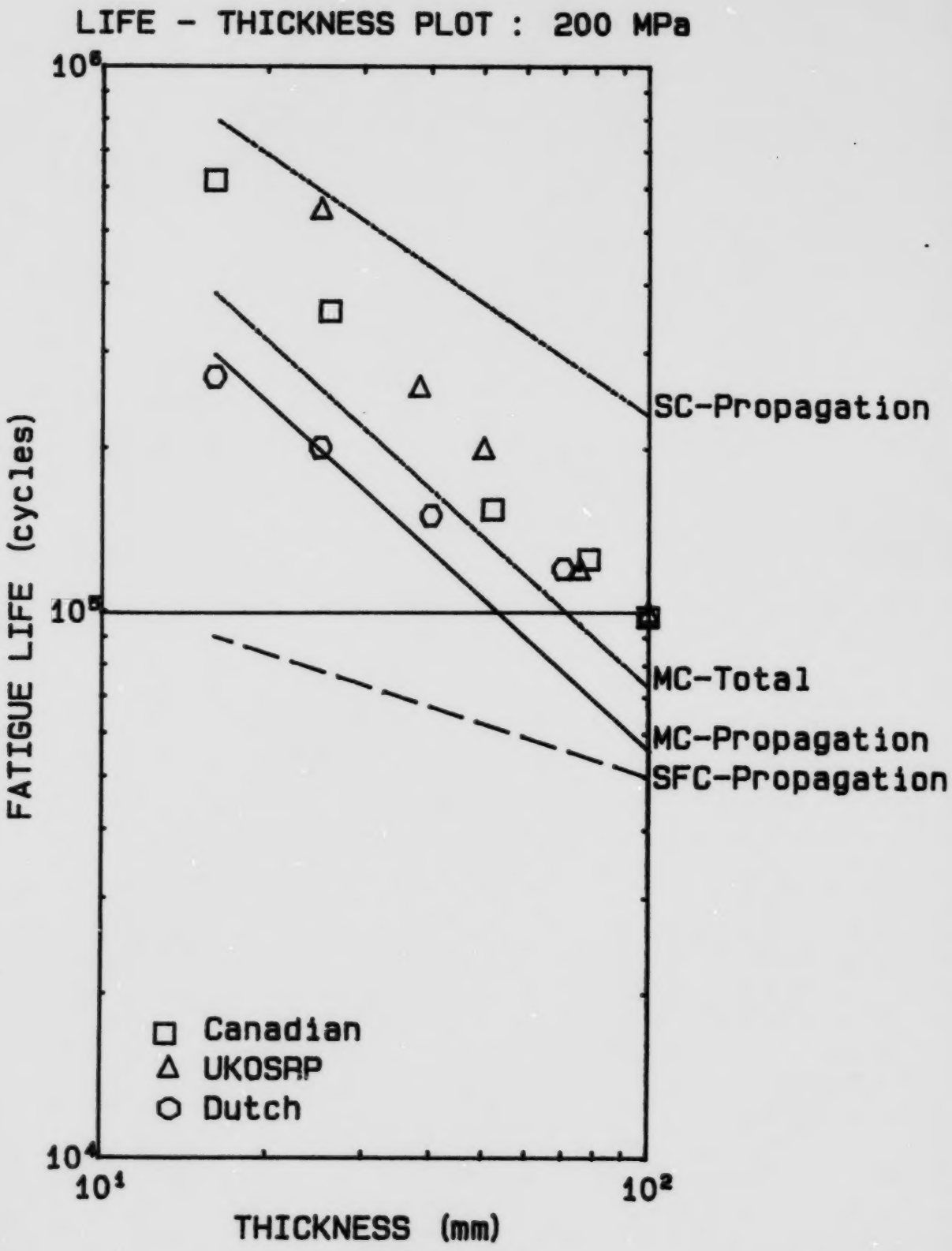
LIFE - THICKNESS PLOT : 200 MPa
10^6
10^5
10^4
10^1
10^2
FATIGUE LIFE (cycles)
THICKNESS (mm)
SC-Propagation
MC-Total
MC-Propagation
SFC-Propagation
Canadian
UKOSRP
Dutch

FIGURE 2.6

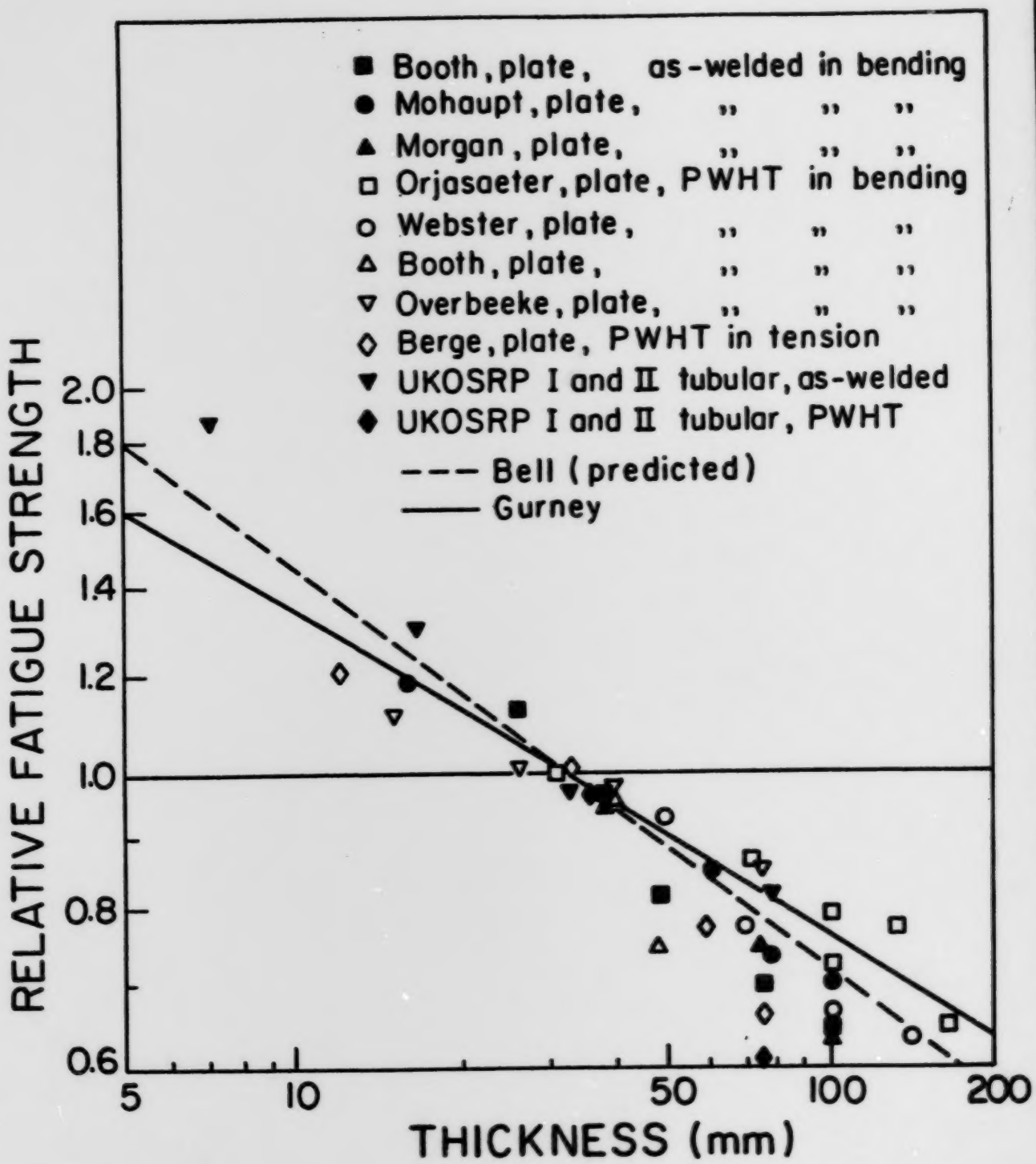

RELATIVE FATIGUE STRENGTH OF "T" PLATE JOINTS

FIGURE 2.7

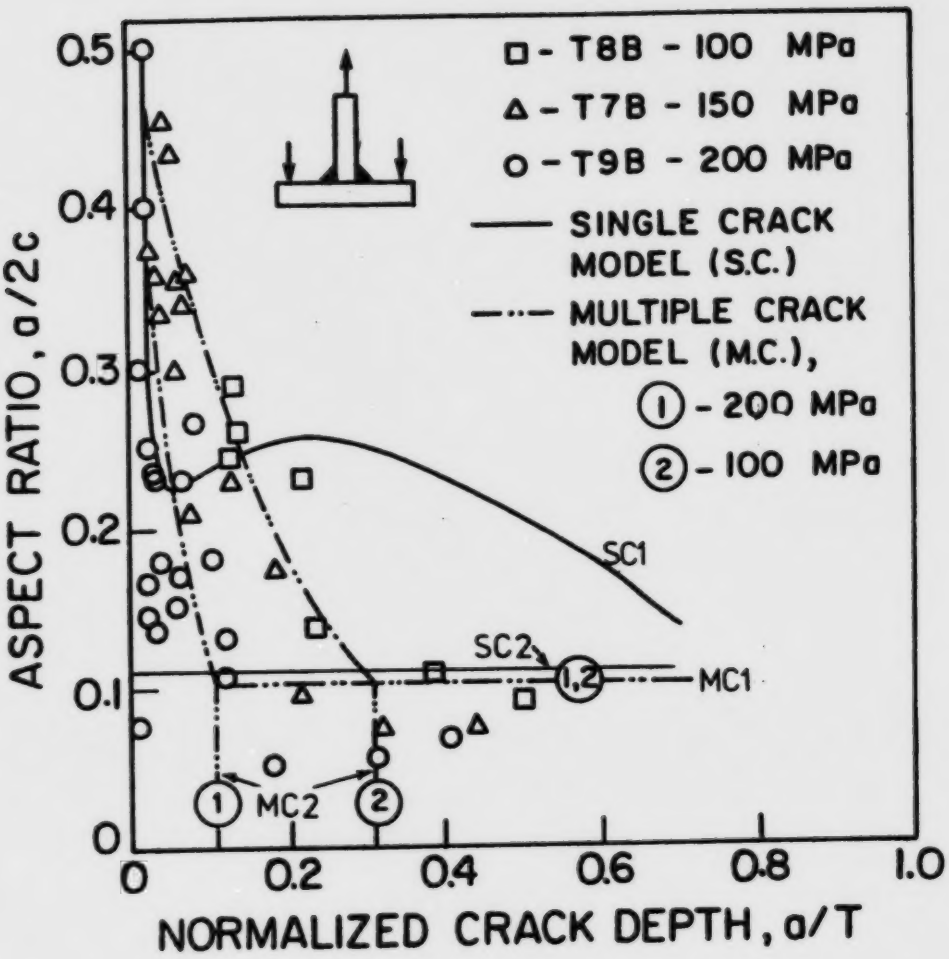
□ - T8B - 100 MPa
△ - T7B - 150 MPa
○ - T9B - 200 MPa
SINGLE CRACK MODEL (S.C.)
MULTIPLE CRACK MODEL (M.C.),
① - 200 MPa
② - 100 MPa
SC1
SC2
MC1
1,2
MC2
ASPECT RATIO, a/2c
NORMALIZED CRACK DEPTH, a/T
0.5
0.4
0.3
0.2
0.1
0
0.2
0.4
0.6
0.8
1.0

FIGURE 2.8

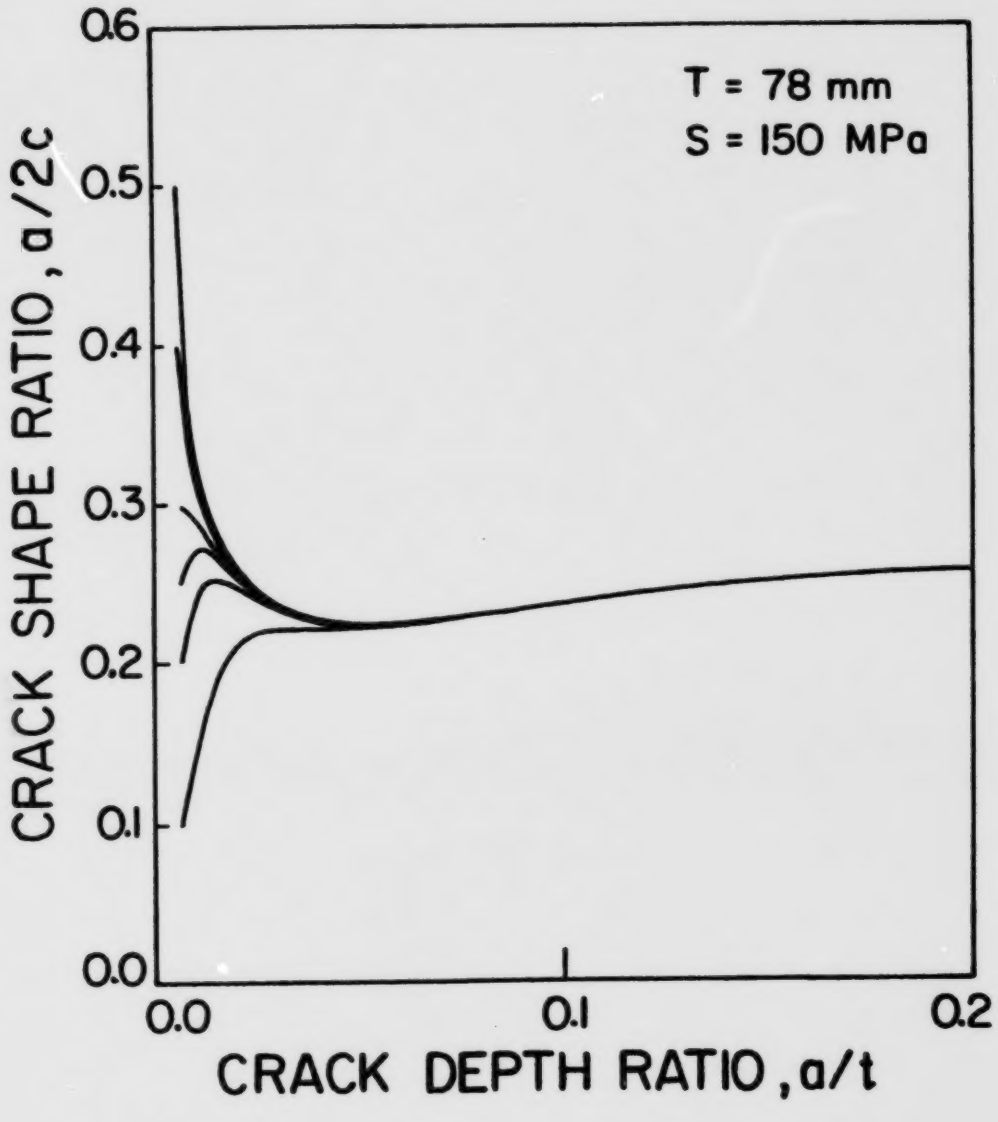
T = 78 mm
S = 150 MPa
CRACK SHAPE RATIO, a/2c
0.6
0.5
0.4
0.3
0.2
0.1
0.0
0.0
0.1
0.2
CRACK DEPTH RATIO, a/t

FIGURE 2.9

3. VARIABLE AMPLITUDE LOADING

3.1 Introduction

Many engineering structures are subjected to complex load environments and it has been shown that the variation in the magnitude of the load cycles effects the fatigue life significantly. In the case of offshore structures the variable amplitude loading applied to the structure by the waves over the anticipated operating life of 20 years will subject the structure to about 10^8 cycles of stress variation and this is the main cause of fatigue cracking. The loading spectrum to which these structures are subjected is extremely complex and the prediction of the load history is very difficult. Also to date there has been very few measurements taken on the response of real structures to confirm or support the prediction techniques used for deriving a variable loading spectrum for fatigue testing. In is for these reasons that there has been a long and difficult debate in Europe over which spectrum characteristics should be used in variable amplitude fatigue tests.

The different testing laboratories in the participating countries in the ECSC program have incorporated different spectrum characteristics in their variable amplitude tests [14]. To remedy this situation and to enable comparisons to be made between tests at different laboratories a "Common Load Sequence" was described by a number of experts within Working Group II of ECSC. It was agreed that this sequence should be employed in Phase III of the ECSC offshore steels program by all laboratories carrying out variable amplitude tests. The Canadian program on variable fatigue tests will use this loading sequence.

This section of the report will discuss the modification of the life prediction program described in section 2.1 to include a variable amplitude loading option. This load option will use the Common Load Sequence of the ECSC program.

3.2 Modifications to Life Prediction Program

The work statement of Phase III of the contract required that the life prediction program described in section 2.1 be modified to include the capability of variable amplitude loading. Also required was the capability to calculate the Miner cumulative damage sum, $\Delta\sigma_{EQ}$, and $\Delta\sigma_{RMS}$ for experimental fatigue test data.

3.3 Variable Amplitude Loading.

At present the prediction program has been modified to include two methods of applying variable amplitude loading:

1. Block Loading
2. Common Load Sequence Loading

In the block loading approach a series of blocks of constant amplitude loading is applied as shown in Figure 3.1 to simulate a variable amplitude loading situation. In the program it is possible to describe up to 50 blocks of constant amplitude loading and to specify the number of cycles in each block. The blocks are applied in the order in which they are specified. An output from the program to a block loading input would be of the form shown in Figure 3.2.

It should be remembered that this technique to approximate variable amplitude loading is a very simplified approach and that the sequence effects are ignored. In many cases of real load histories the sequence effects can be very important because of tensile overloads and crack retardation. In such cases the exact load history must be considered and this requires a detailed step by step analysis.

The Common Load Sequence approach was incorporated by modifying the program to read in the peak and trough stress values for each cycle. These values of stress are supplied by the Common Load Sequence generation program produced by IAGB, Germany. This load sequence will be described in the next section.

The fatigue life is then predicted using a model developed by Barsom [15] which relates fatigue crack growth rate per cycle to an effective stress intensity factor that is characteristic of the probability density curve of the stress history. This model is designated the rms (root mean square) model.

This model attempts to correlate data obtained under constant amplitude and variable amplitude random sequence load spectra. This correlation was found on the basis of the root mean square of the load distribution, where the root mean square is the square root of the mean of the squares of the individual load cycles in the spectra. It is therefore assumed that the fatigue crack growth rate per cycle, da/dN, under variable amplitude loading can be represented by

$$\frac{da}{dN} = A(\Delta K_{rms})^n \tag{3.1}$$

where A and n are constants and

$$\Delta K_{rms} = \sqrt{\frac{\sum_{i=1}^{k} \Delta K_i^2}{k}} \tag{3.2}$$

Therefore the average fatigue crack growth rate can be predicted from equation (3.1) in the same way as the constant amplitude load case.

The prediction procedure for variable amplitude loading is performed in the program in the following manner:

A value of k, (equation 3.2) is chosen over which the root mean square will be calculated

The peak and trough values of stress are read into the program from the common load sequence data file

A value of ΔK is calculated for each stress cycle

The ΔK_{rms} value is calculated for k reversals of stress using equation (3.2)

The average fatigue crack growth increment is calculated for ΔK_{rms} by integration of equation (3.1)

A new series of k stress cycles of stress is read in from the common load sequence data file and the above procedure is repeated

Several test cases have been analyzed using this procedure to illustrate the various prediction models available within the program. These results are described in section 3.6.

3.4 Common Load Sequence.

The common load sequence was developed in the IABG laboratory in Ottobrunn, Germany and described in detail in [16]. The complete common load sequence consists of 5×10^6 load cycles, (10^7 reversals). The overall spectrum is supposed to be a straight line in a half logarithmic scale built up of seven stationary Gaussian spectra of different rms values and numbers of cycles. The seven levels and the overall spectra are shown in Figure 3.3.

The complete common load sequence consists of 5×10^6 cycles, however if it is required that the testing period be shortened to save costs or time it is possible to omit cycles below the 15% level since these small load cycles do not influence the test results. Using the 15% omission level the small rms level is completely omitted and this leads to a return period of 5×10^5 cycles which is 1/10 of the original sequence.

Two other options are available from the common load sequence generation program. The options which are of interest are:

1. Positive peak loads only

This option suppresses the generation of the negative troughs which reduces the storage required for the load sequence. In this case the respective troughs must then be externally generated.

2. Zero Underload

Using this option all the troughs are set to zero which means that all the cycles of the sequence have a value of R = 0.

3.5 Cumulative Damage

A basic assumption made in fatigue investigations which involve spectrum loading is that operation at any given cyclic stress amplitude will produce damage and the seriousness of that damage is related to the number of cycles of operation at that stress level. It is also assumed that damage produced at different stress levels in the sequence will result in an accumulation of total damage equal to the sum of the damage at the individual stress levels. When the damage reaches a critical value failure occurs.

Palmgren [17] and Miner [18] proposed a linear damage rule which states that the damage at any stress level is linearly proportional to the ratio of the number of cycles of operation at that stress level to the number of cycles that would produce failure at that stress level; i.e.

$$D_i = n_i/N_i \tag{3.3}$$

where D is the damage fraction, n is the number of cycles at the given stress level and N is the number of cycles to failure at the same stress level.

The Miner-Palmgren damage rule states that failure occurs when

$$\sum_{j=1} \frac{n_j}{N_j} \geq 1 \tag{3.4}$$

The above linear damage rule was incorporated into the life prediction program. The n_j value is calculated by integration of the growth law for the ΔK_{rms} value within the block as shown in section 2.1 for constant amplitude loading. The number of cycles to failure at this stress is calculated from the F curve (design line) equation for "T" plates obtained from the Department of Energy Guidelines [25] and given by

$$\log(N) = \log(0.63 \times 10^{12}) - 3 \times \log(\Delta\sigma) \tag{3.5}$$

The Miner sum is then calculated using equation 3.4. This procedure has been included in the life prediction program. For a particular load sequence the cumulative damage is calculated at the end of the prediction run. An example of this portion of the output is shown in figure 3.4. In many cases, particularly for long lives the Miner Summation gives values in excess of 1.0 therefore further investigation of this damage rule is continuing together with investigation of other damage accumulation rules.

3.6 Variable Amplitude Loading Predictions

In order to test the life predictions made by the program for variable amplitude loading a series of computer runs were carried out using the "T" plate specimen geometries described in Section 2.3. In each case the load sequence was supplied by the Colos sequence which was modified to give the required rms stress level. The block size k, of equation 3.2, was taken as 1000 cycles in all the following predictions. The computing was performed on an FPS attached processor in order to minimize the computation times.

The results for three rms stress levels of 80, 108 and 150 MPa and the five prediction models described in Section 2.2 are shown in Tables 3.1 - 3.3. It should be noted that the stated rms stress levels are an average value for each thickness because the actual rms stress level which depends on the total number of cycles varies slightly (about ± 2%) for each prediction model.

In Table 3.2 several experimental test results for variable amplitude loading of "T" plates are included and it can be seen that the preliminary indication is that the predictions are quite acceptable. It appears that the SC2 model gives a remarkably good prediction. This model does not account for coalescence but maintains a constant crack shape throughout the propagation phase of the life. It is interesting to note that preliminary observations from the experimental tests are that the coalescence phase of the life is much shorter that was the case for constant amplitude loading.

Further experimental results are required before any conclusions can be made regarding the accuracy of the prediction models for variable amplitude loading.

TABLE 3.1

LIFE PREDICTIONS FOR "T" PLATES USING VARIABLE AMPLITUDE LOADING
σ_{rms} = 80 MPa

t (mm)	Life at t/2 (kcycles)					
	SFC	SC1	SC2	MC1	MC2	EXPT.
26	1234	8210	4641	7149	3680	
52	793	5662	2882	3650	2164	
78	788	4672	2164	2325	920	
103	732	3812	1547	1729	799	

TABLE 3.2

LIFE PREDICTIONS FOR "T" PLATES USING VARIABLE AMPLITUDE LOADING
σ_{rms} = 108 MPa

t (mm)	Life at t/2 (kcycles)					
	SFC	SC1	SC2	MC1	MC2	EXPT.
26	522	4004	1751	2752	1375	1800
52	302	2335	1233	1405	597	
78	291	1911	829	1021	313	800
103	261	1729	637	708	273	

TABLE 3.3

LIFE PREDICTIONS FOR "T" PLATES USING VARIABLE AMPLITUDE LOADING
σ_{rms} = 150 MPa

t (mm)	Life at t/2 (kcycles)					
	SFC	SC1	SC2	MC1	MC2	EXPT.
26	220	750	750	751	263	
52	189	768	273	374	192	
78	189	667	262	263	162	
103	179	526	232	253	141	

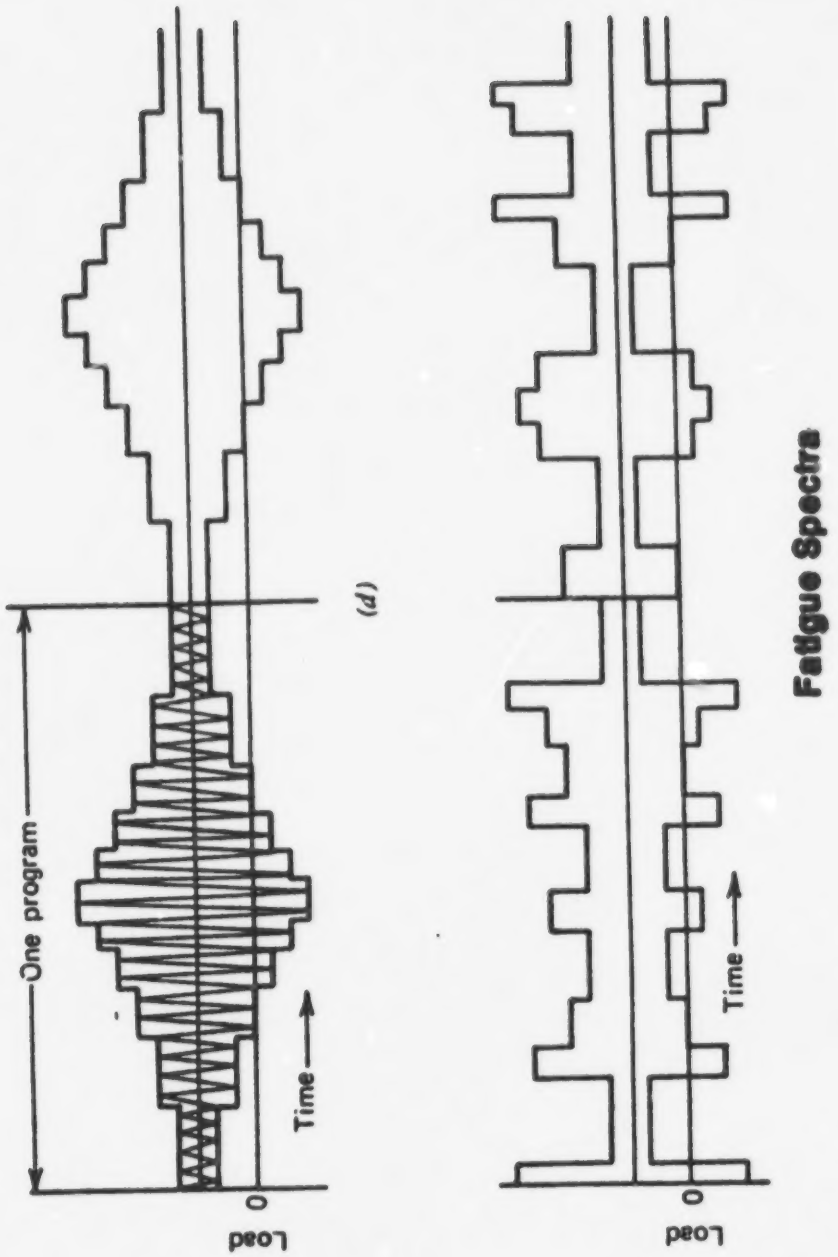

FIGURE 3.1

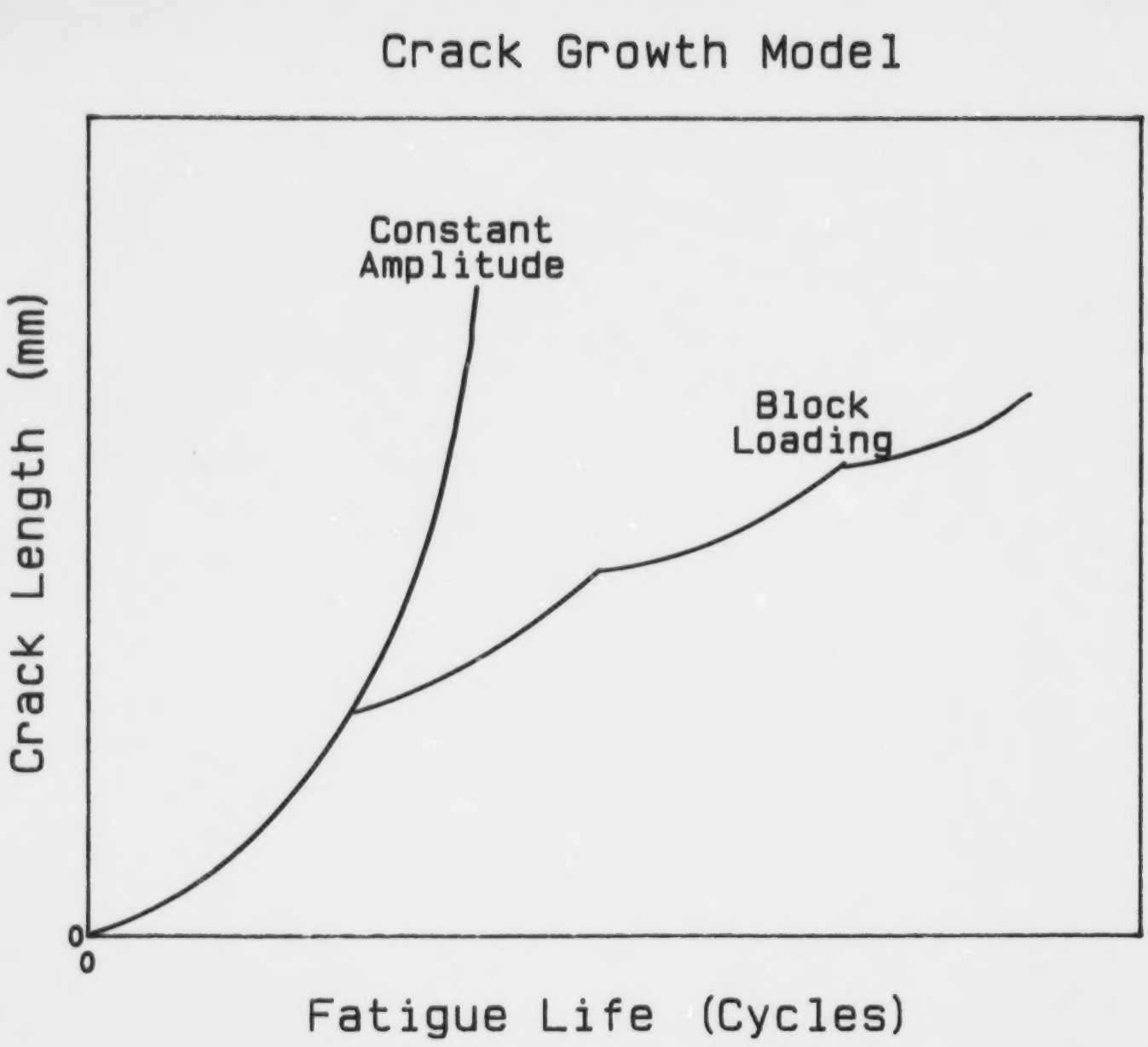
Crack Growth Model
Constant
Amplitude
Block
Loading
Crack Length (mm)
0
0
Fatigue Life (Cycles)

FIGURE 3.2

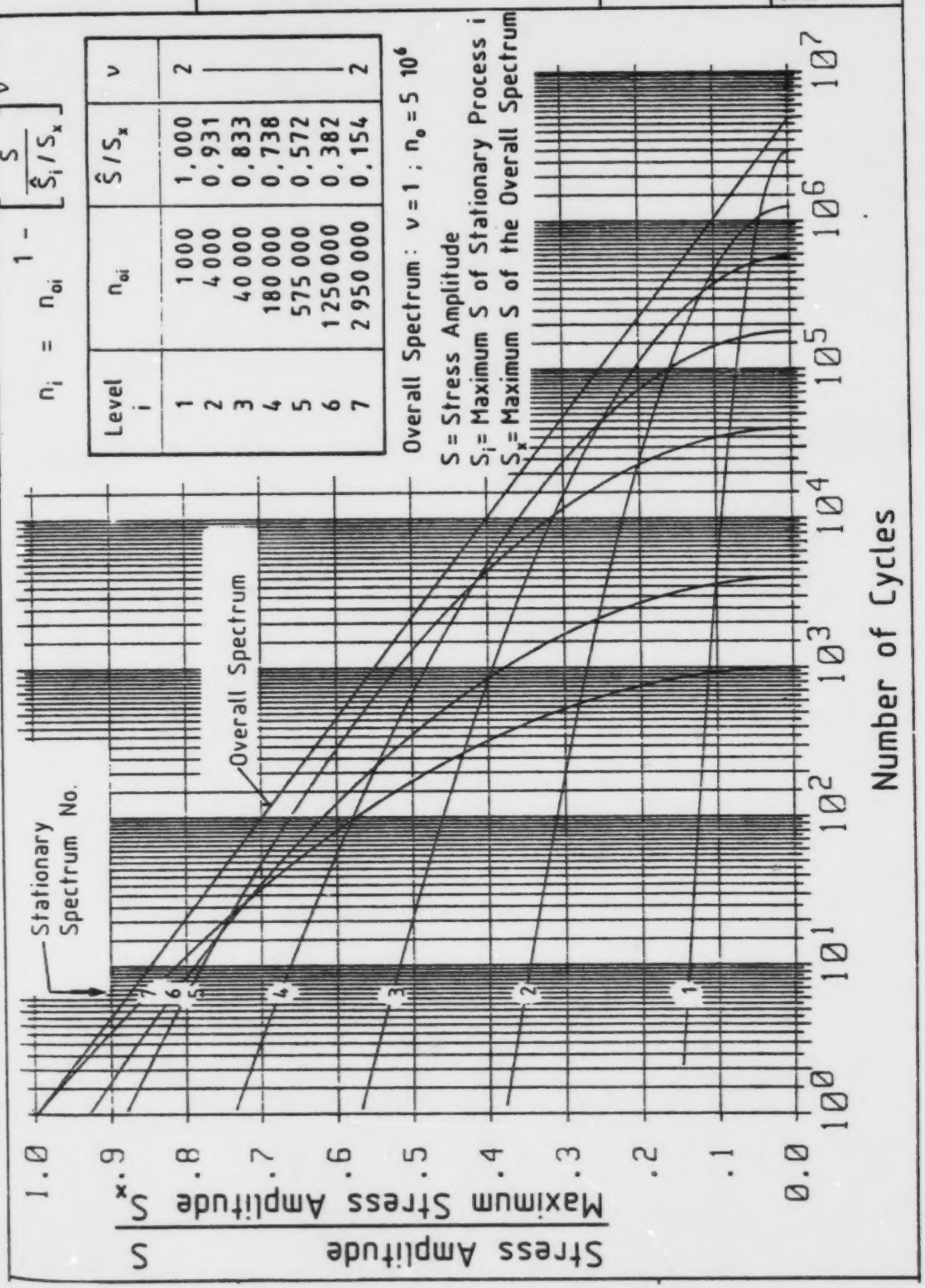
Stress Amplitude S
Maximum Stress Amplitude S_x
Number of Cycles
Stationary Spectrum No.
Overall Spectrum
$n_i = n_{oi}^{1 - \left[\frac{S}{\hat{S}_i / S_x}\right]^v}$
Overall Spectrum: v = 1 ; $n_o = 5\ 10^6$
S = Stress Amplitude
S_i = Maximum S of Stationary Process i
S_x = Maximum S of the Overall Spectrum

Level i	n_{oi}	$\hat{S} / S_x$	v
1	1 000	1,000	2
2	4 000	0,931	—
3	40 000	0,833	—
4	180 000	0,738	—
5	575 000	0,572	—
6	1 250 000	0,382	—
7	2 950 000	0,154	2

FIGURE 3.3

DAMAGE CALCULATION
USING MINER SUMMATION

9 Stress Blocks

Block	Cycles	Stress	Ni	Damage
1	151882	82.9800	1102604.	0.137748
2	88390	116.4694	398753.	0.221666
3	24572	160.2315	153143.	0.160452
4	6235	206.2437	71812.	0.086824
5	1484	252.2212	39264.	0.037795
6	359	298.0078	23804.	0.015081
7	80	343.8991	15490.	0.005165
8	17	389.5510	10657.	0.001595
9	5	440.0124	7395.	0.000676

Total Cycles = 273024 Total Damage = 0.667002

Rms Value of Stress = 109.6100

OUTPUT FROM MINER SUMMATION PROGRAM

FIGURE 3.4

4. STRESS DISTRIBUTION NEAR A WELD TOE

4.1 Introduction

To meet the requirement of the work statement a series of stress analyses were performed on uncracked "T" joints having a range of thicknesses from t = 16 mm to 103 mm and having weld toe radii ranging from r = 0.2 mm to 10.0 mm. The purpose of these analyses was to investigate the stress distribution near the weld toe and the assess the effect of the weld toe radius on the stress concentration factor, (SCF) at the root of the weld toe notch. For each case the nominal weld angle was 45^0, the weld leg length was t/2 and the length of the joint, L was 300 mm as shown in Figure 4.1.

The joints were modelled using ASAS QUM8 isoparametric finite elements and the loading was 3-point bending. In each case the applied load at the vertical plate was adjusted so that the nominal stress σ_x at the weld toe was unity. The finite element mesh was highly refined at the weld toe to insure a smooth radius at the root of the notch.

To meet the requirements of the work statement 5 different plate thicknesses each with 7 different fillet radii were analyzed. The radii used along with the respective plate thicknesses are shown in Table 4.1.

Also a smaller series of analyses were performed to investigate the effect of attachment thickness on the stress distribution near the weld toe notch. In this series of analyses the plate thickness was 52 mm, the weld toe radius ratios were r/t = 0.02 and 0.2 and two values of plate thickness ratios of t_2/t_1 = 0.5 and 0.25 were investigated.

4.2 Stress Concentration Factors

The analyses were performed using the finite element program ASAS_H08 which determined the local nodal stresses and displacements. The postprocessor ASASPOST was also used to calculate the principal stresses and to flag the maximum stress in the mesh. This maximum stress corresponds to the SCF at the weld toe. The results of these calculations are presented in Table 4.2.

Also shown in Table 4.2 are results carried out in Phase I of the contract for a weld toe radius of r = 0.0. (ref. Phase I report section 4.4). It can be seen that the Phase I results for r/t = 0.0 are slightly higher than the present results. This is so because the Phase I results were extrapolated back to the weld toe whereas the present results were not.

To investigate the effect of attachment plate thickness on the SCF at the weld toe notch a series of FE analyses were carried out on a model with base plate thickness, t_1, with vertical attachment thicknesses of t_2/t_1 = 0.5 and 0.25, for r/t ratios of 0.02 and 0.2. The geometry is illustrated in Figure 4.1.

The results from this limited investigation and including the previous case of $t_2/t_1 = 1.0$ are shown in Table 4.3. It can been seen from these results that the value of SCF is reduced with decreasing attachment thickness, about 20% for the range considered. It was noted from these analyses that the position of the stress concentration moved from point A for the r/t =0.02 case to point B in the r/t =0.2 case as shown in Figure 4.2.

4.3 Correlation of SCF's with Empirical Relationships

Lawrence et al. have carried out a great deal of work on the estimation of fatigue crack initiation life of weld using low cycle fatigue concepts, [19] - [21]. In 1981 they proposed a simple relationship between the weld toe radius, the plate thickness and the elastic stress concentration factor, K_t.

$$K_t = \alpha \sqrt{(t/r)} + 1 \qquad (4.1)$$

where K_t is the SCF
t is the thickness
r is the notch root radius
α is a loading and geometry dependant factor

The value of the parameter α has been found for bending and tension loading and is in the range $\alpha = 0.38 - 0.40$.

The average SCF data obtained from the present finite element study for each weld toe radius ratio was compared with the values calculated from equation (4.1). The results are shown in Table 4.4 and plotted in Figure 4.3.

In can be seen from Table 4.4 that the SCF values predicted by the Lawrence equation are in quite close agreement with the present finite element results. This is also evident from the value of α calculated for the average SCF value for each value of r/t. Except for very large radii represented by r/t = 0.5 equation 4.1 give correct SCF values to within 4.7%. This would indicate that equation 4.1 may not be valid for large weld toe radii.

4.4 Fatigue Notch Factor

The results obtained for the stress concentration at the weld toe notch can be expressed in terms of a fatigue notch factor, K_f for zero mean stress and long life, (10^7 cycles). This factor is a way of quantifying the effect of the notch on the stress field and it takes into account the non-Hookeian behaviour caused by yielding at the root of the notch by applying an empirical constant to the Hookeian elastic stress concentration factor, K_t.

Neuber [22] has proposed the following approximate formula for notch factor:

$$K_f = 1 + \frac{K_t - 1}{1 + \sqrt{(a/r)}} \tag{4.2}$$

where a is the Neuber Length
r is the notch root radius
K_t is the elastic SCF
K_f is the Notch fatigue factor.

In this approach Neuber considers a small volume of material at the root of the notch, denoted by the length a, over which the stress can be averaged. This depth of material is called the Neuber Length and its value depends on the material. The Neuber length for various steels is given below [23].

Yield Strength (MPa)	500	1000	2000
Neuber Length a (mm)	0.25	0.08	0.0002

Neuber Length for Steels

Peterson [24] proposed a similar equation for notch fatigue factor:

$$K_f = 1 + \frac{K_t - 1}{1 + \sqrt{(p/r)}} \tag{4.3}$$

where p is a characteristic length similar to the Neuber Length which can be calculated from:

$$p = 2.5 \times 10^{-5}(2068/S_{ult})^{1.8} \tag{4.4}$$

where S_{ULT} is the ultimate tensile stress in MPa.

Equations (4.3) and (4.4) both indicate that large notches with large root radii will have a value of K_f that is almost the same as K_t. However, for small root radii the value of K_f can range from slightly greater that K_t for tough materials to much greater that K_t for brittle materials.

The stress analysis results for the weld toe notch radii considered in this work have been used to calculate the notch fatigue factors according to equations (4.2) - (4.4).

These results have been plotted as Figures 4.4 and 4.5. In these calculation the ultimate tensile strength of an offshore steel was assumed to be approximately 500 MPa which results in a value of the Peterson constant p = 0.322 mm and the Neuber Length a as approximately 0.25 mm.

In can been seen from these plots that the notch fatigue factor K_f for a sharp weld toe notch (ie. r = 0) is much less than the maximum value. This effect was also shown in the work of Lawrence [21] and is due to the fact that under this condition, (r = 0) the notch is no longer a notch but a sharp crack. The maximum value of K_f has been shown by Lawrence to occur when r = p, the Peterson constant which is also shown to be true for the present results.

4.5 Stress Distribution Near the Weld Toe

From the FE analyses carried out to obtain the stress concentration factors reported in section 4.2 the stress distribution in the base plate was plotted. At this stage only the limited investigation of the 52 mm plate with attachment thickness ratios of t_2/t_1 = 1.0, 0.5 and 0.25 and weld toe radius ratios of 0.2 and 0.02 are presented. In all cases the applied load was adjusted so that a nominal stress of 1 MPa was obtained at the weld toe.

In Figures 4.6 - 4.11 the variation of σ_x in the surface of the base plate along the x direction are plotted for the above geometries. The origin of x is taken as the intersection of the base and attachment plates as shown in Figure 4.2, as point B.

In Figures 4.12 - 4.17 the variation of σ_x through the base plate thickness in the y direction in the plane of the weld toe, (section A-A, Figure 4.1), were plotted for the above geometries. In this case the origin of y is the weld toe.

TABLE 4.1

Plate Thicknesses and Weld Toe Radii

t(mm)	15.0	26.0	52.0	78.0	100.0
r/t	Radius (mm)				
0.00	0.00	0.00	0.00	0.00	0.00
0.02	0.30	0.52	1.04	1.56	2.00
0.05	0.75	1.30	2.60	3.90	5.00
0.10	1.50	2.60	5.20	7.80	10.00
0.15	2.25	3.90	7.80	11.70	15.00
0.20	3.00	5.20	10.40	15.60	20.00
0.50	7.50	13.00	26.00	39.00	50.00

TABLE 4.2

Stress Concentration Factors for "T" Plates with Various Weld Toe Radii

* t(mm)	15.0	28.0	53.0	78.0	103.0
* SCF	3.29	3.22	3.38	3.44	3.51
r/t	SCF				
0.00	3.07	3.09	3.13	3.18	3.23
0.004	6.21	6.20	6.20	6.21	6.21
0.010	4.57	4.60	4.68	4.77	4.85
0.02	3.55	3.58	3.63	3.70	3.76
0.05	2.78	2.80	2.86	2.90	2.9
0.10	2.22	2.24	2.27	2.30	2.33
0.15	1.97	1.98	2.09	2.08	2.06
0.20	1.79	1.80	1.82	1.85	1.88
0.50	1.40	1.40	1.40	1.41	1.42

* - Phase I results

TABLE 4.3

Variation of SCF with Attachment Thickness for a Base Plate Thickness of 52 mm

t_2/t_1	r/t	SCF
1.0	0.02	3.63
0.5	0.02	3.39
0.25	0.02	2.93
1.0	0.2	1.82
0.5	0.2	1.73
0.25	0.2	1.56

TABLE 4.4

Comparison of FEM SCF Values with those Predicted by the Lawrence Equation

FEM Calculations			Lawrence Equation
r/t	Avg. SCF	α	SCF ($\alpha = 0.4$)
0.00	3.14	-	-
0.02	3.64	0.37	3.82
0.05	2.85	0.41	2.79
0.10	2.27	0.40	2.27
0.15	2.03	0.40	2.03
0.20	1.83	0.37	1.89
0.50	1.41	0.29	1.57

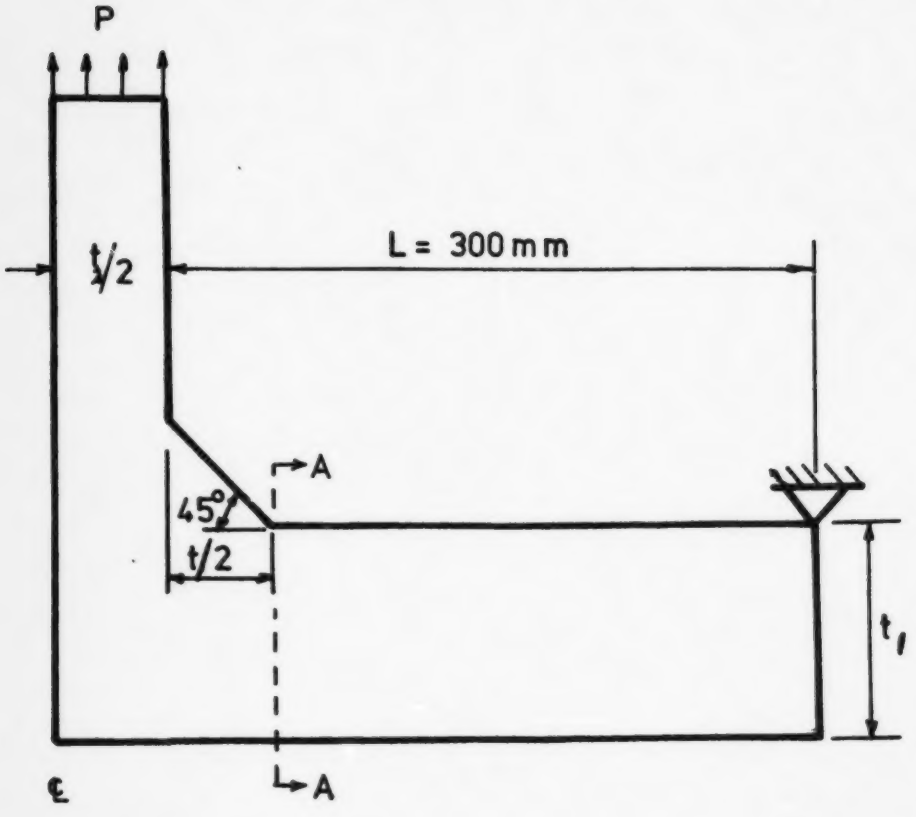

FIGURE 4.1

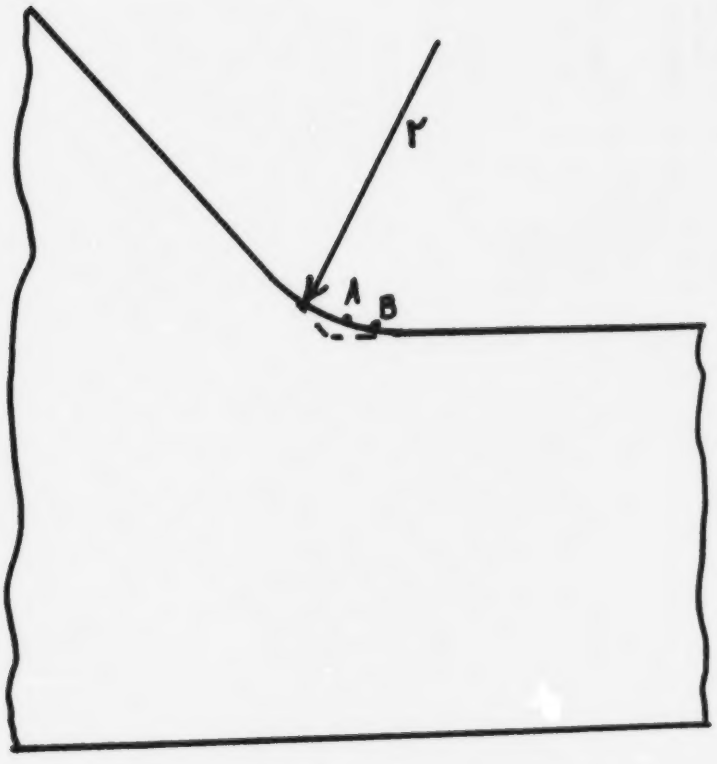

FIGURE 4.2

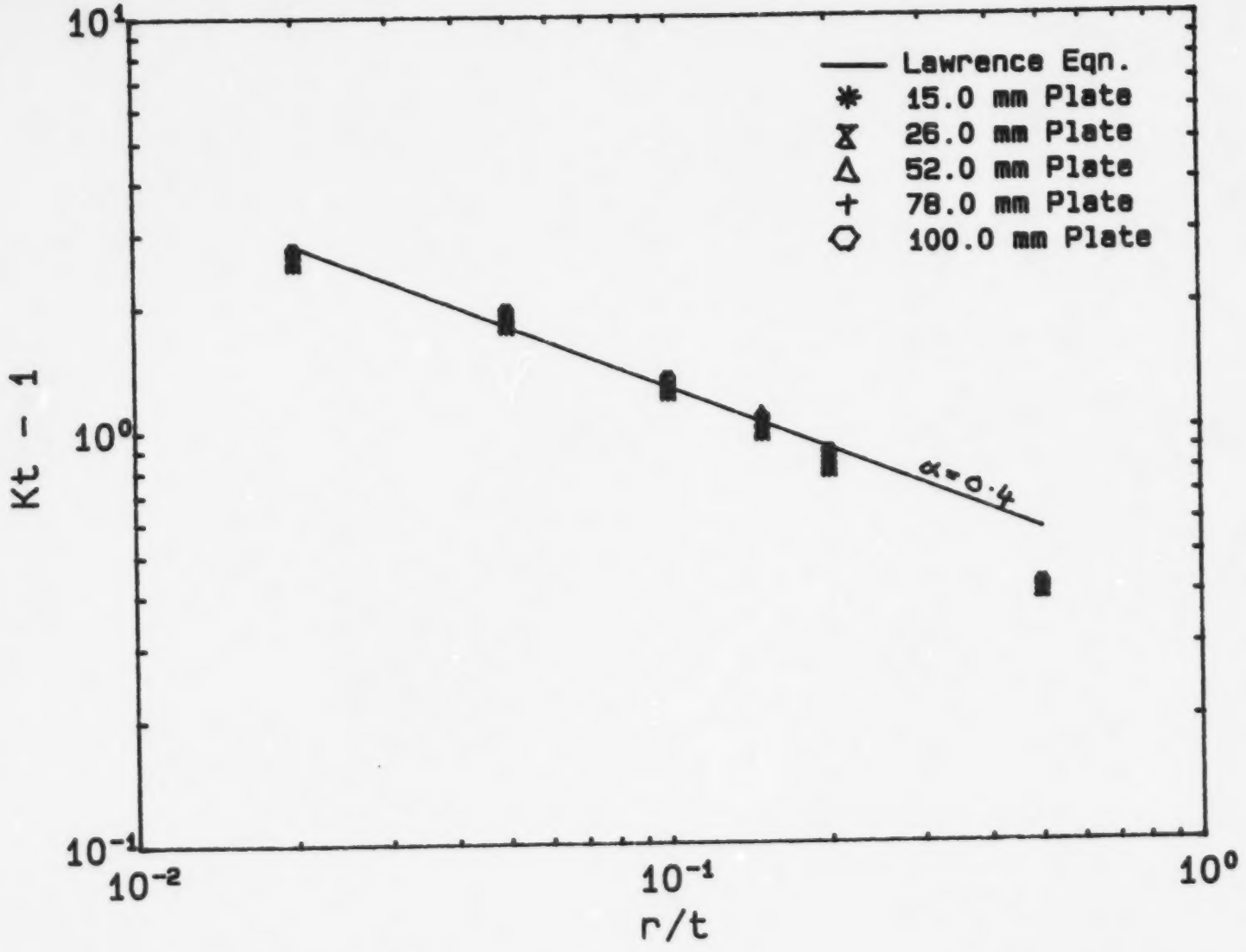

FIG. 4.3 - SCF Values From ASAS_H and the Lawrence Eqn.

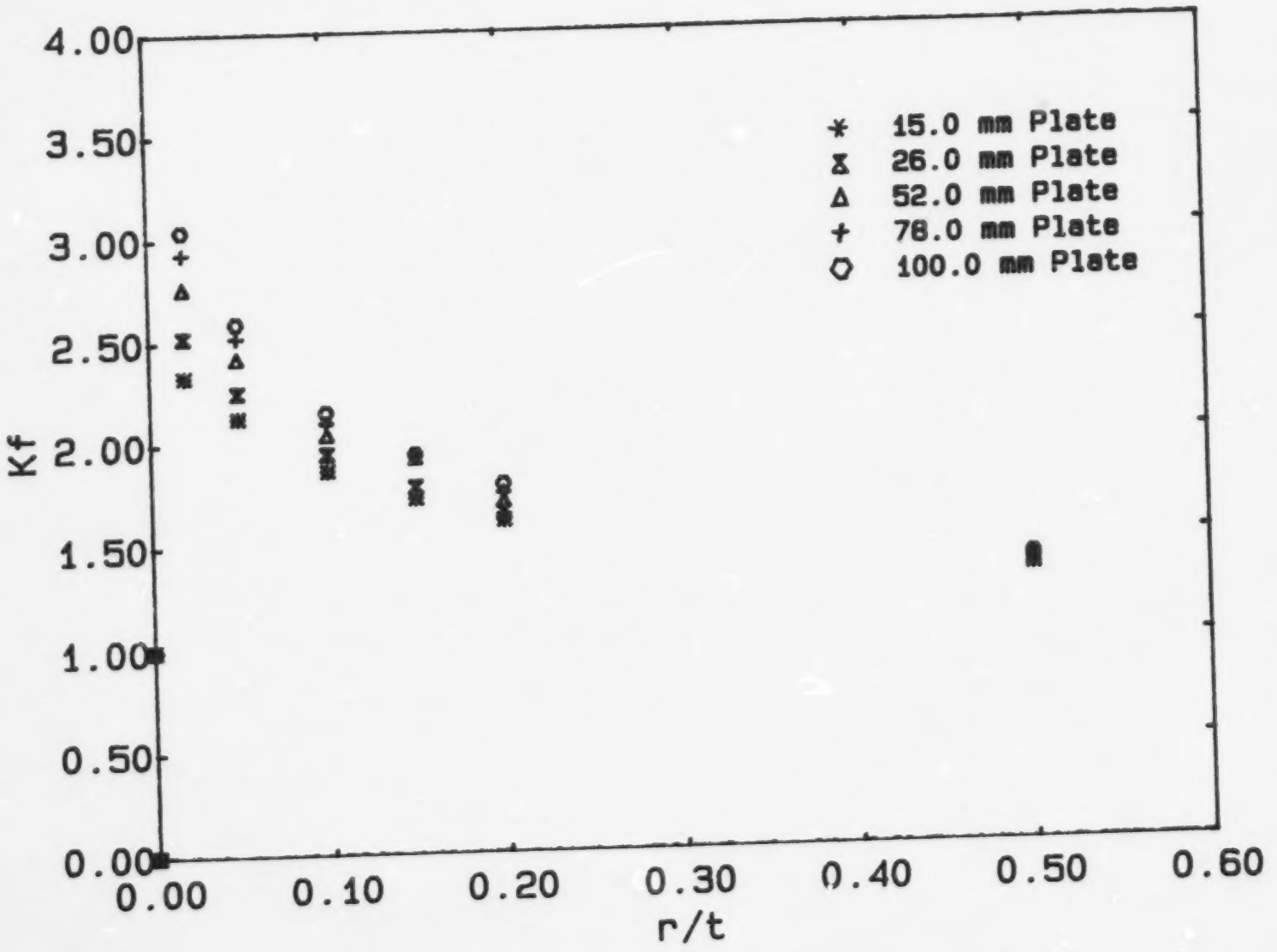

FIG. 4.4 - Kf Values From ASAS_H and the Neuber Equation

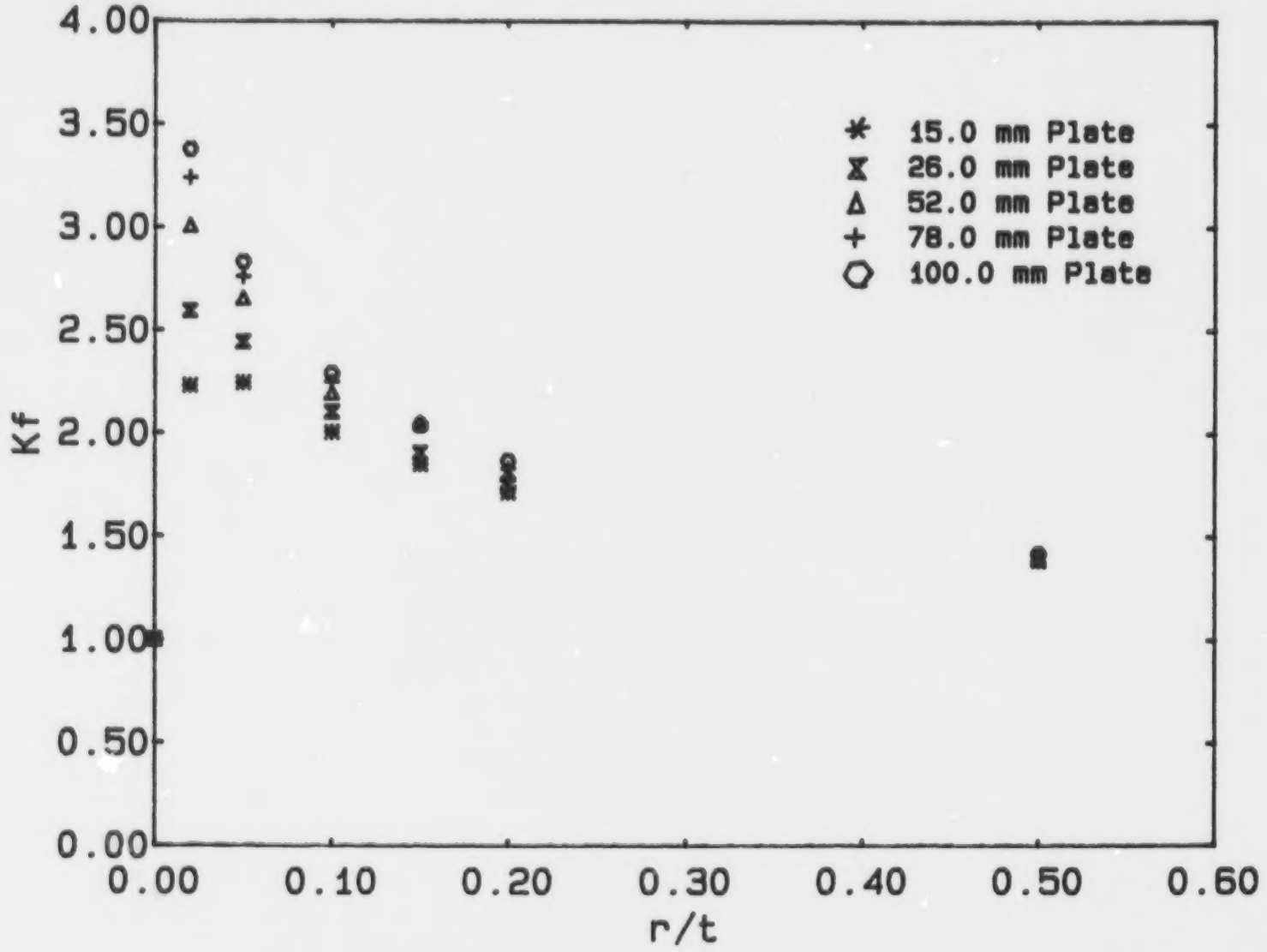

FIG.4.5 - Kf Values From ASAS_H and the Peterson Equation

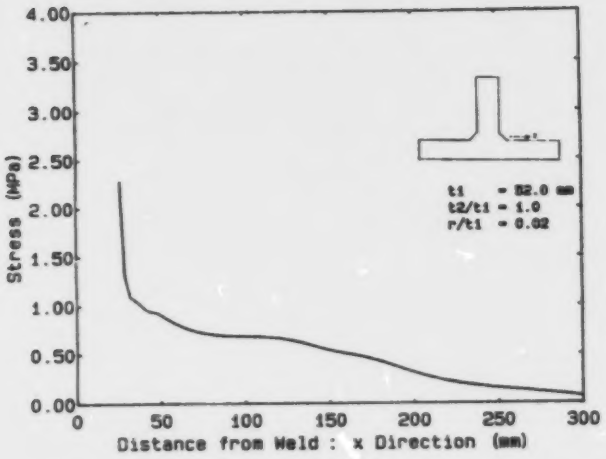

FIGURE 4.6

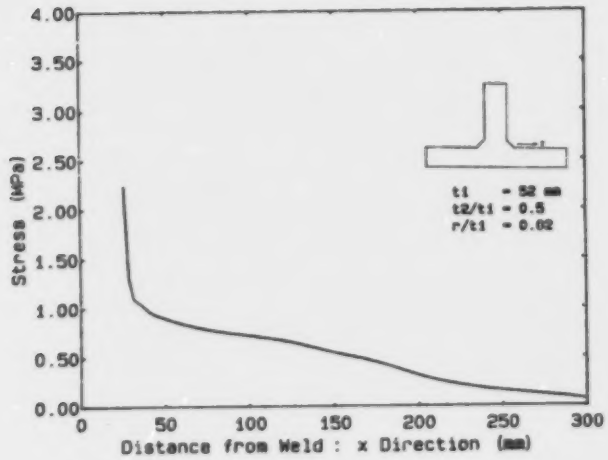

FIGURE 4.7

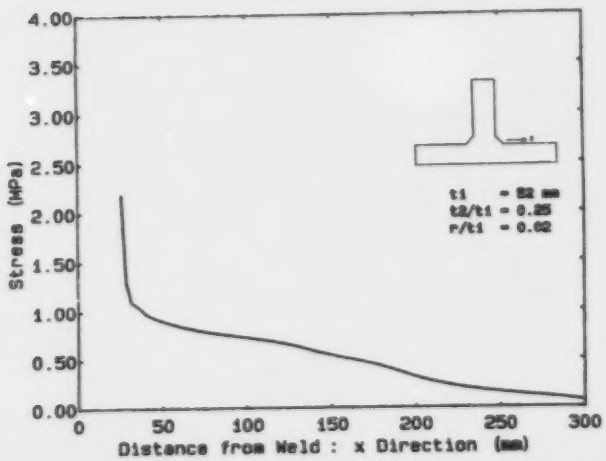

FIGURE 4.8

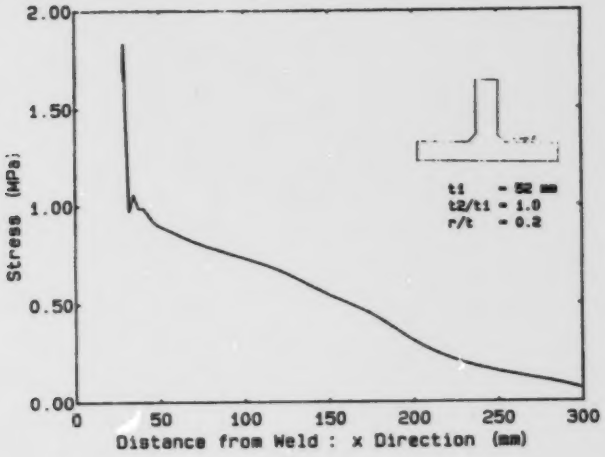

FIGURE 4.9

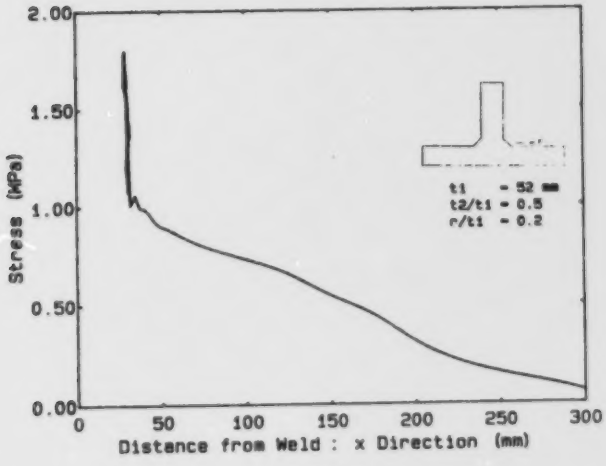

FIGURE 4.10

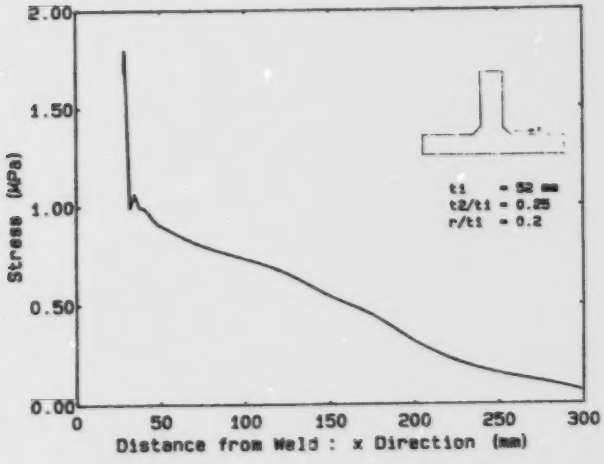

FIGURE 4.11

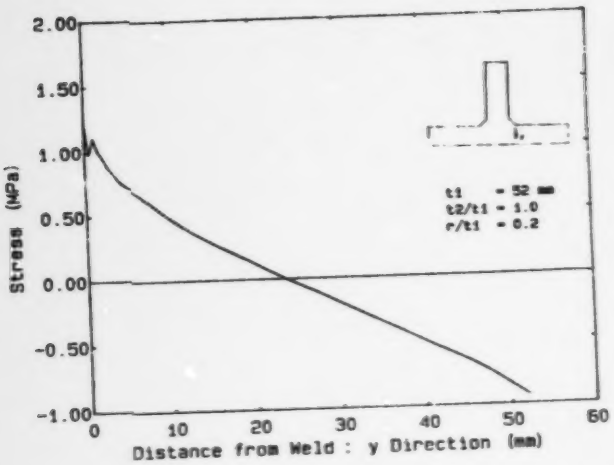

FIGURE 4.12

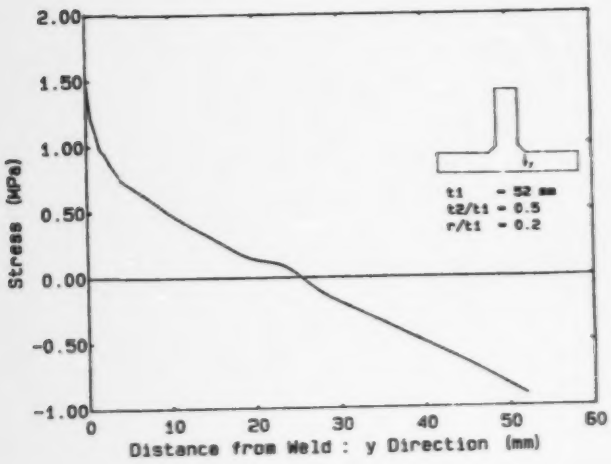

FIGURE 4.13

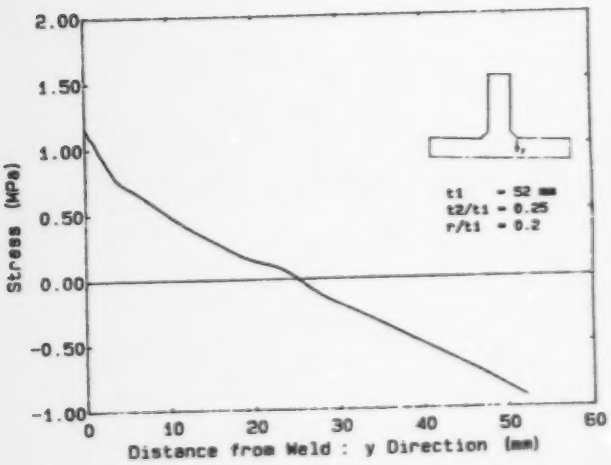

FIGURE 4.14

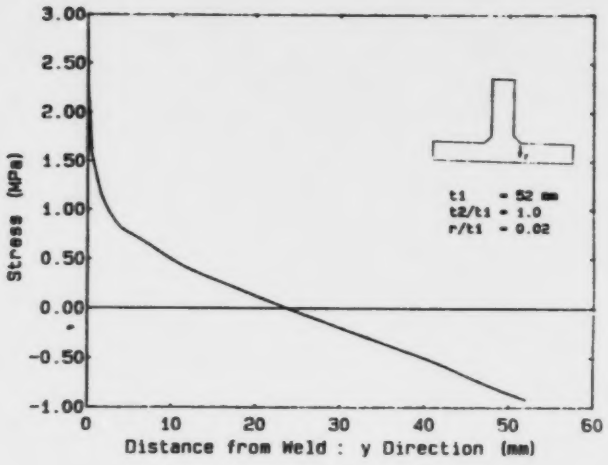

FIGURE 4.15

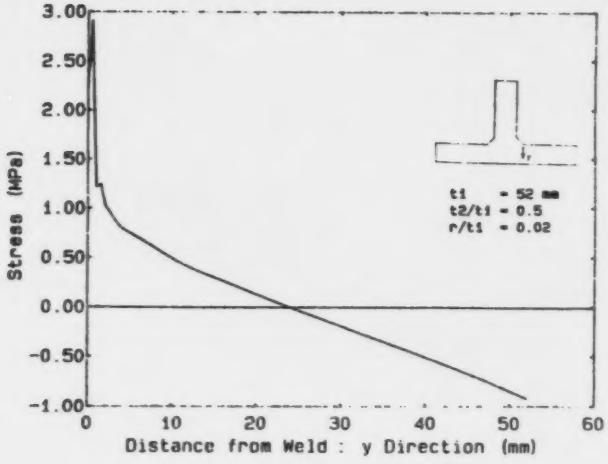

FIGURE 4.16

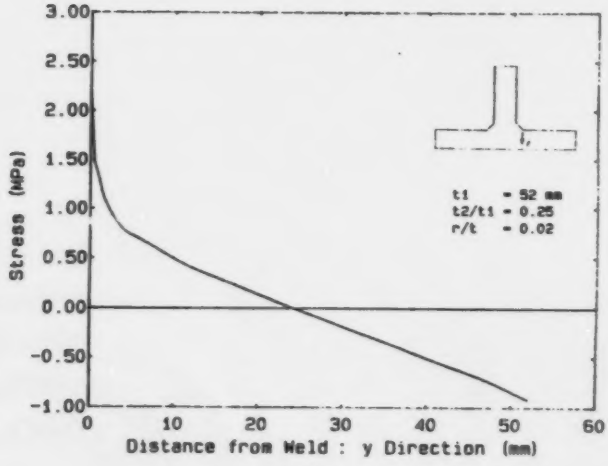

FIGURE 4.17

5. FINITE ELEMENT ANALYSIS OF PIPE-TO-PLATE JOINTS

5.1 Introduction

In an amendment to Contract OST85-00428 dated November 20, 1987 a requirement to investigate the procedure for the determination of stress intensity factors (SIF's) of cracks at the weld toe of pipe-to-plate joints using finite elements was stipulated. This section of the report describes the methodology for carrying out this work.

5.2 Pipe-to-Plate Joint

The pipe-to-plate joint was developed at the University of Waterloo to investigate the fatigue behaviour of welded joints in offshore structures. This specimen was developed to be an intermediate step between the testing and analysis of plate to plate joints, ("T" plate joints) and pipe to pipe tubular joints. The advantages of this specimen compared with the tubular joints are cost and ease of analysis.

The pipe-to-plate joint is shown in place on a test fixture in Figure 5.1. The specimen consists of a 26 mm thick plate of dimensions 1020 x 1520 mm to which is welded a 457 mm diameter pipe of 30 mm wall thickness. Under test the pipe is loaded perpendicular to its axis and the plate is clamped in such a way to produce the require stress distribution at the weld toe.

This specimen geometry, testing procedure and the results of several tests of this specimen are described in detail in [27].

5.3 Methodology for Finite Element Analysis

The goal of this work is to develop a procedure to model and calculate the SIF of a weld toe crack in a pipe-to-plate joint using finite elements. To carry out this analysis the modelling procedure used to model and calculate the SIF's at semi-elliptical weld toe cracks welded "T" plate joints will be followed and extended where required. The general outline of this procedure was described in Phase II report of this contract [2].

In this modelling procedure the multilevel substructuring capability of the ASAS finite element program is used extensively and where possible the individual substructure are produced by mesh generation programs [2]. To model a pipe-to-plate specimen with a semi-elliptical weld toe crack, Figure 5.2(a), only one half of the specimen need be modelled due to symmetry as shown in Figure 5.2(b). This 180^{o} section of the specimen is in turn made up of segments as shown in Figure 5.3. The angular size of these segments are chosen such that uncracked segments of the model can be progressively replaced by segments containing a crack region so that specimens containing longer cracks around the weld toe can be modelled without repeating the solution of the entire finite element mesh.

Each of the above segments are produced in a similar way as the mesh for welded "T" plate joints. Individual segments are modelled using 5 substructures as shown in Figure

5.4 and each substructure is produced by a mesh generation program. Typical finite element meshes for the substructures containing a crack (i.e. substructures 2 and 3) are shown in Figure 5.5. As before the crack tip region will be modelled using finite elements which incorporate the $1/\sqrt{r}$ stress singularity at the crack tip.

When the above substructures are produced they are linked together to form the complete pipe-to-plate joint. The model is then solved and the SIF for the modelled crack shape is calculated from the displacements as described in [1]. Using this procedure it will be possible to replace individual substructures and thus model difference crack shapes which will result in substantial savings of computer time and cost.

The above modelling procedure is a complex undertaking and the analysis is proceeding in a step by step fashion. To date the mesh generation programs have been modified and the base plate substructures have been produced, linked together and solved. This model describes a curved semi-elliptical surface crack in a plate. Work is now underway to add the weld and pipe substructure to the model and to complete the pipe-to-plate model by adding the remaining angular segments.

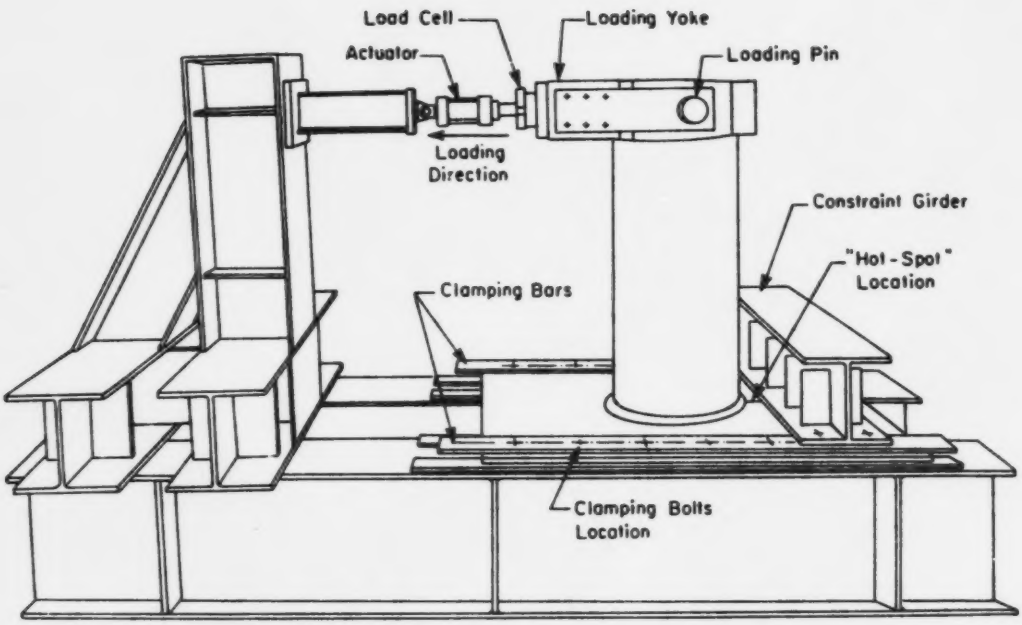

TEST RIG FOR PIPE-TO-PLATE JOINT

FIGURE 5.1

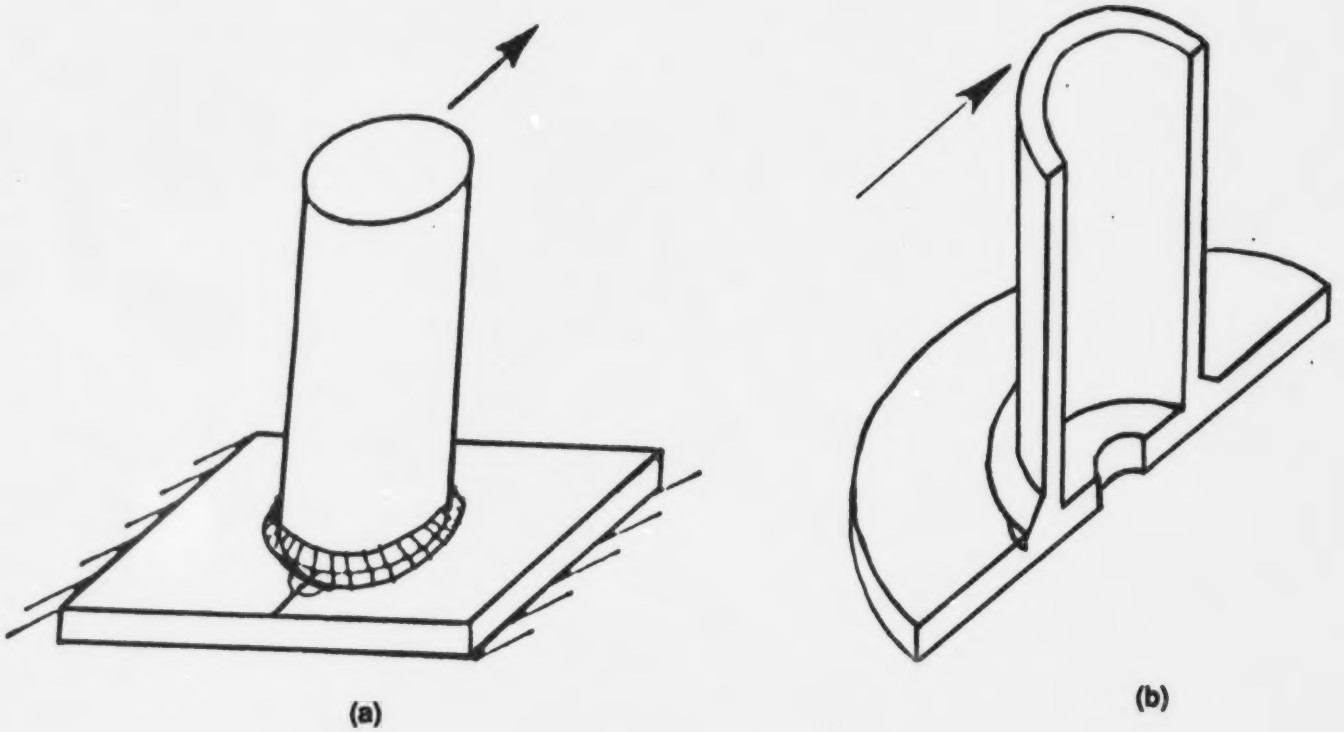

PIPE-TO-PLATE JOINT

FIGURE 5.2

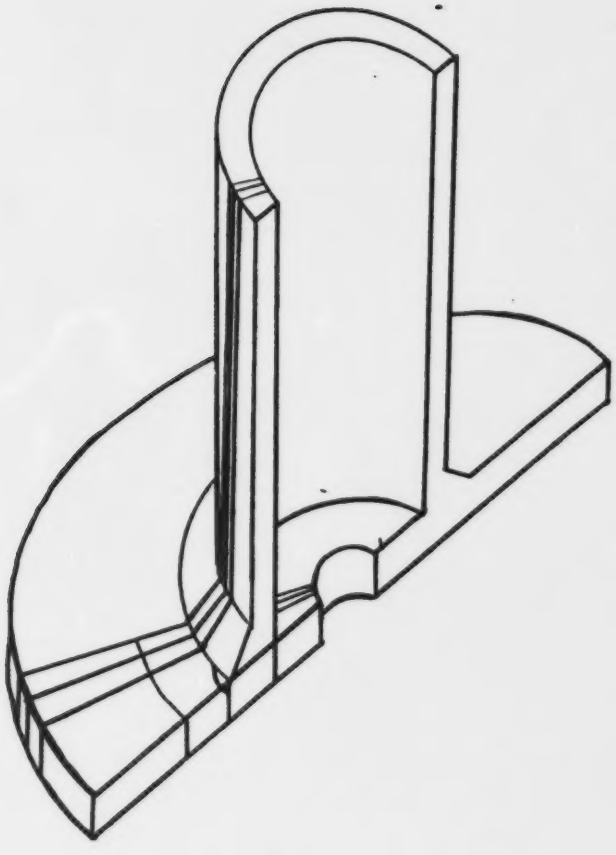

SUBSTRUCTURE ANALYSIS

FIGURE 5.3

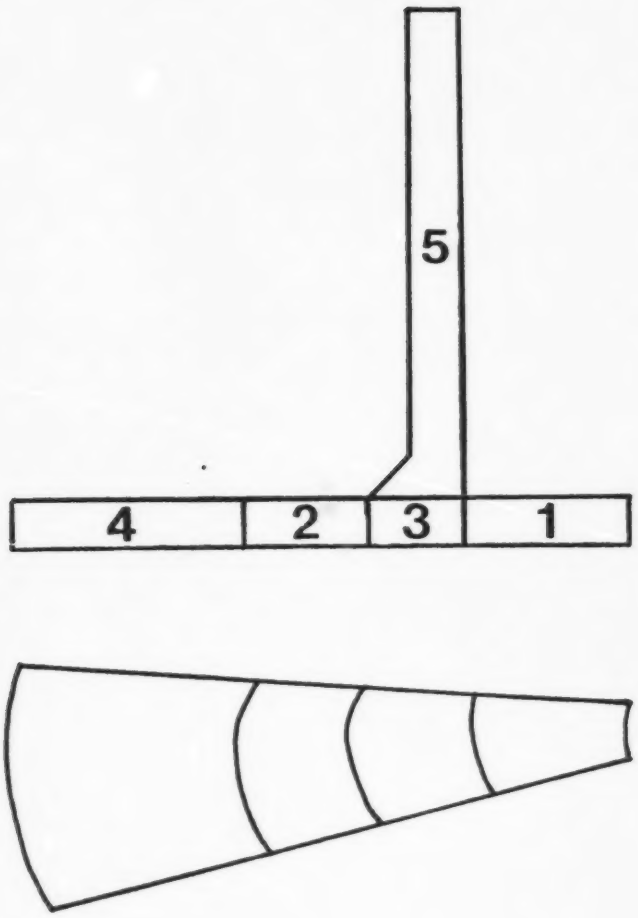

SUBSTRUCTURE ANALYSIS

FIGURE 5.4

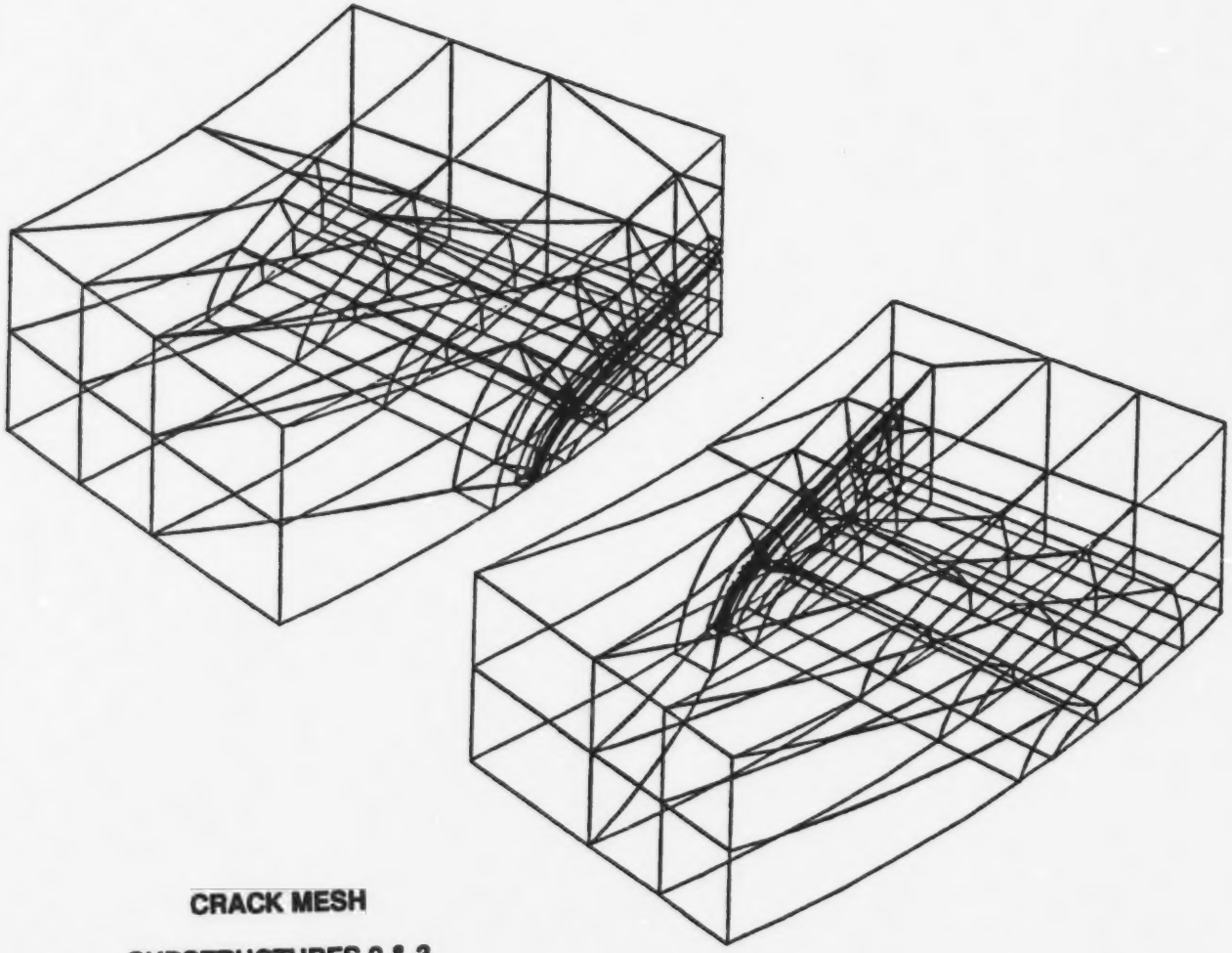

CRACK MESH

SUBSTRUCTURES 2 & 3

FIGURE 5.5

6. REPORT ON CANADA-ECSC MEETINGS

6.1 ECSC Progress Meeting Riso, Copenhagen.

The principal investigator attended the ECSC progress meeting held in the Riso National Laboratory, Copenhagen, Denmark during April 23-24, 1986. This trip was financed from travel funds from within Carleton University.

At this meeting I made a presentation on our work in Canada on Prediction of Fatigue Crack Growth at Weld Toes using Fracture Mechanics and participated in group discussions. I also attended the International Planning Committee, (IPC) of the conference Steels in Marine Structures to be Held in Delft, The Netherlands in June 1987.

My overall feeling on the Progress and IPC planning meetings, from a Canadian perspective was very favourable. In the presentations and numerous discussions it was evident that the Canadian Offshore Research Program was accepted by the other participants as making a valuable contribution to the body of knowledge on the behaviour of steels in marine structures.

On returning to Canada I am a brief written report on my trip to PMRL which I have included as Appendix III. I also make a verbal report on these meetings to PMRL on May 1986.

6.2 Canada -ECSC Progress Meeting, Halifax, Nova Scotia.

The principal investigator participated in a Canada-ECSC Group Progress meeting in Halifax, Nova Scotia on September 29, 1986 and also attended the Conference "Cathodic Protection: A + or - in Corrosion Fatigue" on September 30. This conference was sponsored by CANMET. At the progress meeting I made a presentation reporting on our current work on Fracture Mechanics analysis of offshore steels.

Also included in this trip was a visit to Memorial University, St. Johns, Newfoundland to attend a meeting of the participants in the Canadian Offshore Steels research program. This meeting was attended by representatives of PMRL, AMCA International, Memorial University, Waterloo University and Carleton University.

6.3 Contract Progress Meetings.

The principal investigator visited the University of Waterloo on February 19-20, 1987 to finalize the contents of the papers being submitted by the participants in the Canadian offshore steels research program to the Conference on Steels in Marine Structures which will be held in Delft, The Netherlands, June 1987.

The principal investigator hosted a contract progress meting at Carleton University Ottawa on August 13-14, 1987.

The principal investigator also attended a meeting at the University of Waterloo to finalize a paper which was presented at the OMAE conference in Houston, Texas in February 1988 [26].

6.4 Conference on Steels in Marine Structures, Delft, 1987.

The principal investigator is planning to attend the conference on Steel in Marine Structures to be held in Delft, The Netherlands on June 15-18, 1987 to present the paper A Fracture Mechanics Model for Life Prediction of Welded Plate Joints which is included as Appendix II.

7. CONCLUSIONS

1. The work outlined in the Contract work statement has been successfully carried out.

2. The fatigue crack propagation life of welded "T" plate joints under constant amplitude loading has been predicted and compared with experimental data.

3. The stress concentration factors (SCF) and stress distribution for welded "T" plate joints with varying thickness, weld angles and weld toe radii have been obtained.

4. The fatigue life prediction program has been modified to include the capability of predicting the fatigue life of welded joints subjected to variable amplitude loading. The load history used was the Colos sequence and the predicted results were compared with the available experimental data.

5. The Miner damage accumulation rule has been incorporated in the life prediction program.

6. The principal investigator attended contract progress meeting and presented a paper at the conference on Steels in Marine Structures in Delft, the Netherlands in June 1987.

8. REFERENCES

1. **R. Bell and J. Kirkhope,** "Determination of Stress Intensity Factors for Weld Toe Defects". (D.S.S. Contract OSU82-00233, Phase I Report, Faculty of Engineering, Carleton University, Ottawa, 1984).

2. **R. Bell,** "Determination of Stress Intensity Factors for Weld Toe Defects". (D.S.S. Contract OST84-00125, Phase II Report, Faculty of Engineering, Carleton University, Ottawa, 1985).

3. **P.C. Paris and F. Erdogan,** "A Critical Analysis of Crack Propagation Law". (Trans. ASME, J. Basic Eng., Vol. 85, No.4, 1963)

4. **R.G. Forman, V.E. Kearney and R.M. Engle,** "Numerical Analysis of Crack Propagation in Cyclic-Loaded Structures". (Trans. ASME, J. Basic Eng., Vol. 89, No.3, 1967).

5. **J.E. Collipriest,** "An Experimentalist's View of the Surface Flaw Problem. The Surface Crack: Physical Problems and Computational Solution", (ASME, pp 43-62, 1972)

6. **M. Kiensnil and P. Lukas,** "Influence of Strength and Stress History on Growth and Stabilization of Fatigue Cracks". (Engineering Fracture Mechanics, Vol. 4, 1972).

7. **W. Schulz,** "Procedures for Prediction of Fatigue Life of Tubular Joints". (Intl. Conf. on Steel in Marine Structures - Special and Plenary sessions, Paris, 1981).

8. **T.R. Gurney and G.O. Johnston,** "A Revised Analysis of the Influence of Toe Defects on the Fatigue Strength of Transverse Non-Load-Carrying Fillet Welds", (Welding Institute International, 9-3, 1979).

9. **J.C. Newman and I.S. Raju,** "An Empirical Stress Intensity Factor Equation for a Surface Crack", (Engineering Fracture Mechanics, Vol. 15, No.1-2, 1981)

10. **G.R. Irwin,** "The Crack Extension Force for a Part - Through Crack in a Plate", (Trans. ASME<, J. of Appl. Mech., Vol. 29, No.4, 1962).

11. **U.H. Mohaupt, D.J. Burns, J.D. Kalbfleisch, O. Vosikovsky, and R. Bell,** "Fatigue Crack Development and Thickness Effects in Welded Plate to Plate Connections", (Proc. Intl. Offshore Conf on Steel in Marine Structures, Paper TS-3, Delft, June, 1987).

12. **R. Bell, O. Vosikovsky, D.J. Burns and U.H. Mohaupt,** "A Fracture Mechanics Model for Life Prediction of Welded Plate Joints", (Proc. Intl. Offshore Conf. on Steels in Marine Structures, Paper TS-53, Delft, June 1987).

13. **O. Vosikovsky, R. Bell, D.J. Burns and U.H. Mohaupt,** "Fracture Mechanics Assessment of Fatigue Life of Welded T-Joints, Including Thickness Effects", (Proc. of 4th Intl. Conf. on Behaviour of Offshore Structures, (BOSS'85), pp. 453-464, Delft, 1985)

14. **D.J. Burns,** "Design of Experiments to Evaluate the Fatigue and Corrosion Fatigue properties of Welded Structures", (D.S.S. File No. O9SU.23378-2-6298,Department of Energy, Mines and Resources, Ottawa, Canada, 1982)

15. **J.M. Barsom,** "Fatigue Crack Growth Under Variable-Amplitude Loading in ASTM A514 Grade B Steel", (ASTM STP 536, Philadelphia 1973).

16. "The Common Load Sequence for Fatigue Evaluation of Offshore Structures-Background and Generation - ", (IABG Report TF- 1892, Ottobrunn, 1985)

17. **A. Palmgren,** "Durability of Ball Bearings," (ZDVDI, Vol. 68, No. 14, 1924)

18. **M.A. Miner,**"Cumulative Damage in Fatigue",(Trans. ASME, J. Appl. Mech., Vol. 67, 1945)

19. **F.V. Lawrence, R.J. Mattos, Y. Higashida and J.D. Burk,** "Estimating the Fatigue Crack Initiation Life of Welds", (ASTM STP 648, 1978).

20. **F.V. Lawrence and R.J. Mattos,** "Estimation of the Fatigue Crack Initiation Life of Welds Using Low Cycle Fatigue Concepts", (Society of Automotive Engineers, SP-424, 1979).

21. **F.V. Lawrence, N.J. Ho and P.K. Mazumdar,** "Predicting the Fatigue Resistance of Welds, (Annual Review of Material Science, Vol. 11, 1981).

22. **H. Neuber,** "Theory of Stress Concentration for Shear-Strained Prismatical Bodies with Arbitrary Non-Linear Stress-Strain Law", (J. of Materials, Trans. of ASME, Dec. 1961).

23. **H.O. Fuchs and R.I. Stephens,**"Metal Fatigue in Engineering", (John Wiley and Sons, New York, 1980).

24. **R.E. Peterson,** "Stress Concentration Factors", (John Wiley and Sons,New York, 1974).

25. "Offshore Installations: Guidance on Design and Construction, New Fatigue Design Guidance For Steel Welded Joints in Offshore Structures", (U.K. Department of Energy, HMSO, 1984).

26. **R. Yee, D.J. Burns, U.H. Mohaupt, R. Bell and O. Vosikovsky,** "Thickness Effect and Fatigue Crack Development in Welded T-Joints", (Proceedings of the 7th International Conf. on Offshore Mechanics and Arctic Engineering, (OMAE), Houston, 1988, pp 447-457)

27. **S.B. Lambert, U.H. Mohaupt, D.J. Burns and O. Vosikovsky,** "Simulation of Fatigue Behavior of Tubular Joints Using a Pipe-To-Plate Specimen", Proc. Intl. Offshore Conf. on Steels in Marine Structures, Paper TS-18, Delft, June 1987).

28. **R. Bell,** "Stress Intensity Factors for Weld Toe Cracks in Welded "T" Plate Joints"(DSS Contract OST84-00125, Faculty of Engineering, Carleton University, Ottawa, May 1987)

APPENDIX I

WORK STATEMENT

Using the SIF determined in Phase I and the FM model developed in Phase II of the contract, provide the following fatigue life predictions and analyses.

1. Predict fatigue life, using the best available experimental data on crack growth, as a function of thickness for welded joints exposed to cold sea water environment at free corrosion potential, optimum cathodic protection and cathodic overprotection, tested at constant amplitude loading. Calculate fatigue crack growth rate (FCGR) curves from PMRL experimental data on T joints.

2. Predict fatigue life as a function of thickness for welded joints exposed to air and cold sea water environment (with and without cathodic protection) tested under variable amplitude (common) load sequence. Calculate Miner sums, $\Delta\sigma$ equivalent, $\Delta\sigma$ RMS and FCGR curves from PMRL experimental data.

3. Determine the effects of FCGR thresholds (in air and sea water) on S-N curves, and fatigue limit.

4. Determine stress distribution near weld toe for the previously used range of thickness, and weld toe angles, and weld toe radii ranging from 0.2 to 10 mm.

5. The contractor is required to attend an ECSC-Canada meeting held in Halifax in September, 1986 and present a paper at the Conference on Steels in Marine Structures held in June, 1987, in Delft, the Netherlands.

6. Determine stress intensity factor for a semi-elliptical weld toe crack ($\frac{a}{b} = 0.4$; $\frac{a}{c} = 0.25$) in a pipe-to-plate welded joint, using FE analysis.

DELIVERABLES

To be submitted to the Scientific Authority bi-monthly progress reports.

A Draft Final Report to be submitted to the Scientific Authority 30 days before completion. Upon acceptance by the Scientific Authority a Final Report in 20 copies to be submitted on or before February 28, 1988.

The Final Report will contain an executive summary in both English and French.

The CANMET standard cover page must be used.

All reports produced under this contract shall be considered in the public domaine and will be catalogued in the CANMET library.

A Seminar is to be presented on the findings upon completion of the contract.

APPENDIX II

A FRACTURE MECHANICS MODEL FOR LIFE PREDICTION OF WELDED PLATE JOINTS

R. Bell,[1] O. Vosikovsky,[2] D.J. Burns[3] and U.H. Mohaupt[3]

[1]Dept. of Mechanical & Aeronautical Engineering, Carleton University, Ottawa, Canada. K1S 5B6
[2]CANMET/PMRL, 586 Booth Street, Ottawa, Canada. K1A 0G1
[3]Dept. of Mechanical Engineering, University of Waterloo, Waterloo, Canada. N2L 3G1

ABSTRACT

This paper describes the development and testing of a fracture mechanics model for fatigue life prediction of welded plate joints.

Included are numerical investigations of 2-D and 3-D stress intensity factors at the weld toes of welded plates loaded in 3-point and 4-point bending. Of particular interest are the effects of crack geometry, crack depth, shape of weld profile and mode of loading. The numerical studies were performed using the general purpose finite element program ASAS.

Empirical relations for K as a function of the above variables have been established, and are included in a life prediction program for welded plate joints. Also included in this program are empirical relationships developed from experimental results to account for the development, growth and coalescence of multiple cracks.

The life prediction program is validated by comparison of predicted fatigue lives with test results for welded "T" joints with plate thicknesses ranging from 16 mm to 103 mm, loaded through the attachment in 3-point bending under constant amplitude loading. The experimental results are presented in detail in another paper at this conference.

1. INTRODUCTION

During the past number of years there has been an increasing and justified interest in the use of fracture mechanics procedures for estimating the life and the development and propagation of cracks in large offshore structures. Current design practice utilizes the S-N design curve approach and this will remain the primary method of design for some years to come. However, fracture mechanics procedures do present a method of dealing with a tubular structure which contains flaws and demonstrates the influence of a number of variables on the propagation fatigue cracks. Also the testing and analysis of full scale tubular joints is a costly and time consuming undertaking, therefore in many cases the crack propagation behaviour from the weld toe has been studied using welded "T" plate specimens loaded in 3-point and 4-point bending.

This paper describes a fracture mechanics model developed for the prediction of fatigue life and the investigation of fatigue crack propagation and coalescence at the weld toe of welded "T" plate joints as shown in figure 1.

From the Canadian experimental program described in detail in reference [1] and summarized in figure 2 it can be seen that the life of welded "T" plate joints is dominated by fatigue crack propagation and this accounts for about 70% of the life. This crack growth starts at small initial flaws at the weld toe which grow under the influence of cyclic loading into small cracks, which are initially of semi-elliptical shape. These cracks grow deeper and coalesce and finally grow as a single crack until failure of the specimen. Therefore, after making various assumptions on initial crack size and shape it is possible to describe the growth rate of a crack at the weld toe using a linear elastic fracture mechanics (LEFM) approach, in which the growth rate of the crack can be described by a single parameter the stress intensity factor K. In this approach the crack growth rate da/dN is related to the stress intensity range ΔK by a law such as the Paris Law

$$da/dN = C\Delta K^m \quad \ldots\ldots\ldots\ldots\ldots \quad (1)$$

where C and m are material constants, and ΔK is given by

$$\Delta K = Y\Delta\sigma\sqrt{\pi a} \quad \ldots\ldots\ldots\ldots\ldots \quad (2)$$

and Y is a factor describing the geometry. The stress intensity factor, K describes the stress environment at the crack tip and for two different geometries of the same material the stress distribution will be identical if the stress intensities are equal. It follows that the fatigue crack propagation in two bodies will be identical if the cyclic variation in ΔK is the same. The value of K for complex geometries is best obtained using the finite element method and this procedure will be described in section 2.1.

It can be seen from figure 3 that the life of the welded joint can be described by considering three regions. These regions can be designated as (i) initiation, (ii) macro crack coalescence, and (iii) straight fronted crack growth.

Region (i) of the life which is commonly referred to as the initiation phase, includes the initiation of very small cracks on the micro scale, the micro coalescence of these small cracks and the commonly referred to short crack growth region. This region would include cracks up to approximately 0.5 mm. and will not be considered in this paper.

Region (ii) which will be referred to as the macro crack coalescence phase includes cracks of high aspect ratios, a/c, the coalescence of these cracks into fewer cracks of lower aspect ratio and eventually into one dominant semi-elliptical crack. Region (iii) of the life covers the growth of the dominant semi-elliptical crack into a crack of very low aspect ratio and the eventual growth of this crack as a straight fronted crack until final failure. These two regions which describe the propagation life of the joint will be considered in section 3 and will be included in the fracture mechanics model for life prediction of welded joints described herein.

2. FATIGUE CRACK GROWTH MODEL

The fatigue life prediction model developed herein is based on linear elastic fracture mechanics. The above equation (1) can be integrated to give:

$$N = \frac{1}{C} \int_{a_i}^{a_f} da/(\Delta K)^m \quad \ldots\ldots\ldots\ldots (3)$$

Thus the number of cycles N, to propagate a crack from an initial size a_i to a final size a_f, can be calculated. Therefore it is possible to estimate the fatigue life once a solution for K as a function of crack shape and depth is known.

2.1 S.I.F. Determination by FEM

The numerical calculations of SIF were performed using the general purpose finite element program ASAS. Both 2-D and 3-D analyses of the welded joints were carried out. The joints were modelled using quadratic isoparametric elements and the crack tip region by collapsed isoparametric elements which prescribe the $1/\sqrt{r}$ singularity at the crack tip, [2]. The stress intensity factors were evaluated using the classical Westergaard equations for displacements in the vicinity of the crack tip. In order to carry out the analyses at a reasonable cost the multi-level substructuring capabilities of the program were used extensively to perform the analysis for different loadcases and crack geometries.

2.1.1 2-D Solutions for K

A series of 2-D analyses were carried out for crack depth ratios, a/t, varying from 0.02 - 0.5, where a is the crack depth and t is the plate thickness. Three weld shapes were chosen arbitrarily for investigation of the effect of weld shape on the SIF at the weld toe. A 70° weld was chosen to be representative of a severe weld shape, a 45° shape as typical of an actual weld profile and a 30° weld shape as representative of a weld after profiling. The finite element models were loaded in tension, 3-point bending, (load-carrying weld), and also in 4-point bending, (non-load-carrying weld). A typical 2-D finite element mesh is shown in figure 4.

The results obtained from this series of analyses were normalized with respect to K for a plate without a weld and presented in terms of a SIF magnification factor M_k [3]. Curves were fitted to these results to describe the variation of K for the welded "T" plate joint with a straight fronted crack, (SFC). This 2-D solution for K was then included in the life prediction program described in section 4.

2.1.2 3-D Solution for K

Modelling semi-elliptical weld toe cracks in "T" plate joints is both time consuming and the data production is both tedious and error prone. Therefore a mesh generator was developed to produce the required meshes. Also the substructure analysis capability of the finite element program was used to make the series of analyses more cost effective. The calculations were performed for crack shapes in the range

$$1.0 > a/c > 0.25$$

and for crack depths

$$0.025 > a/t > 0.4$$

The loading conditions and the weld shapes

considered were those described in the previous section. A typical 3-D mesh and substructure analysis is shown in Figure 5 (a) and (b).

The SIF results obtained were presented in terms of a SIF magnification factor, M_k, which when multiplied by the SIF for a surface crack in a plate subjected to pure bending, gives the SIF for a weld toe crack as shown in equation (4).

$$K_{I,\ weld} = M_k \times K_{I,\ (pure\ bending)} \quad \ldots\ldots(4)$$

The solution for $K_{I,(pure\ bending)}$ was obtained from the empirical relationship of Newman and Raju [4] for a surface crack.

In order that these results could be included in a life prediction program it was necessary to fit curves to the data. However it was not possible to obtain a simple expression for the variation of SIF because the results vary with both a/c and a/t. Therefore, a method was developed in which bi-cubic spline functions were used to fit a surface to the results. In this procedure the entire surface was represented by bi-cubic spline co-efficients. To evaluate a SIF value one simply has to produce a fundamental B-spline for the particular co-ordinates of the independent variables and multiply it by the appropriate coefficients to obtain the curve fitted value of SIF. Using this procedure it was possible to reproduce the original FEM results to within several percentage points.

In order to compare the 2-D and 3-D SIF's for the "T" plate and to demonstrate the variation of SIF with crack shape, crack depth and weld angle the results were normalized with respect to an embedded circular crack and presented in figure 6. It can be seen from this figure the weld angle only effects the SIF results over the first 10% of the thickness of the plate.

3. CRACK SHAPE DEVELOPMENT

From examination of the ink stains and beach marks on the specimens tested in the experimental program reported in [1] it was found that there was a number of randomly distributed cracks initiated along the weld toe. The number, size and shape of these initial cracks depended on the stress range and thickness of the specimen as shown in figure 7 (a-c). These figures also show the development of the cracks as they grow through the thickness. The small cracks which are initially semi-elliptical coalesce as they grow deeper into a smaller number of cracks with lower aspect ratios, (a/c), until they eventually join into a single almost straight fronted crack (SCF). This crack grows until final failure occurs.

In order to characterize this behaviour in a life prediction program the number and aspect ratios of the cracks are plotted as a function of crack depth for all the specimens tested. It was found that if an assumption was made that the initial very small cracks were semi-circular, the crack shape development as a function of crack depth could be described by the exponential relationship

$$a/c = e^{-ka} \quad \ldots\ldots(5)$$

It was also shown that the parameter k, which describes the variation of mean aspect ratio of the crack with crack depth, could be described by an equation having the same form as Gurney's for fatigue strength [5]. Thus the equation relating the parameter k to the stress range and plate thickness could be stated as follows:

$$k = k_B \left(\frac{\Delta\sigma}{\Delta\sigma_B}\right)^2 \left(\frac{t}{t_B}\right)^{\frac{1}{2}} \quad \ldots\ldots(6)$$

where t_B is a reference thickness and $\Delta\sigma_B$ is the associated stress range, t is any thickness and $\Delta\sigma$ is its associated stress range.

In the present work a reference thickness of 26 mm and a stress range of $\Delta\sigma_B$ of 116 MPa were assumed, which corresponds to a value of $k = k_B = 0.2$. It should be noted that the above empirical equations (5) and (6) were developed for a specific welding procedure and therefore may only be valid for welds with similar weld toe geometries and in a strict sense for similar loading modes.

The above development of the empirical equation for crack shape variation is described in greater detail in [6].

As stated previously, and as shown in figure 3, the region of crack coalescence accounts for a significant portion of the propagation life. Therefore, in order to characterize the effects of crack coalescence on the life of the joint the above empirical equations were incorporated in the life prediction program described in the following section.

4. FATIGUE LIFE PREDICTION PROGRAM

The fatigue life prediction model described in this section is based on LEFM. Using equation (3), the number of cycles N, to propagate a crack from an initial size a_i to final size a_f can be calculated by a cycle by cycle integration of the growth law using a Runge Kutta numerical integration technique.

The relationships obtained for the SIF's, as described in section 2.1 were included in the computer program. Using the 2-dimensional SIF relationship it was possible to predict the growth of a straight fronted crack, hereafter referred to as the SFC case. The growth of a single semi-elliptical crack can be predicted using the expressions for 3-dimensional SIF's. In this case the growth law is integrated on a cycle by cycle basis in the depth direction to obtain the change in crack depth, a, and in the surface direction to obtain the change in crack length, c. Using these values a new elliptical crack shape is found and this procedure is designated the single crack (SC) solution.

However, as stated above it was noted that for crack propagation from a weld the case of multiple initiation and crack coalescence must be considered to accurately describe the propagation life. Therefore equations (5) and (6) were incorporated into the prediction program. To model the crack coalescence behaviour the following procedure was adopted. The initial crack size was chosen and the increase in crack depth a and crack surface length c were calculated as outlined above. To simulate crack coalescence the surface crack length c was updated at each increment of growth using the empirical relationships above. Also, when the crack aspect ratio reached a value of a/c = 0.2, the crack was assumed to be straight fronted and the 2-dimensional SIF solution was used for the remainder of the life. To accommodate the change from semi-elliptical to straight fronted crack growth some local smoothing in the ΔK values was performed. This procedure was designated the multiple crack, (MC) case.

An example of the predictions of the straight fronted, (SFC), the single crack, (SC), and the multiple crack, (MC), cases for a welded "T" plate specimen is shown in figure 8, compared with the experimental results of [1].

It can be seen that the SFC case is conservative, the SC case over predicts the life by a large amount and the MC case, which accounts for the multiple nucleation and coalescence of cracks, gives a good prediction.

5. COMPARISON OF PREDICTED AND EXPERIMENTAL RESULTS

This section of the paper describes the fatigue life prediction results for the welded "T" plate specimens using the computer program described in the previous section.

The specimen geometries considered are those described in [1] and [6] and shown in figure 1. In all cases the specimens were loaded in 3-point bending, the nominal weld angle was 45°, and the multiple crack case was simulated as described in section 3. After study of the results of the experimental program the initial crack size was chosen to be a_i = 0.5 mm, the initial crack shape, a/c was taken to be semi-circular and the life of the specimens was assumed to have expired when the crack reached a depth of a/t = 0.5. The value of initial crack depth was chosen to be 0.5 mm which was considered to be a valid initial condition for the application of LEFM. It should also be noted that this size of initial crack was considered to be the smallest crack that could be repeatably detected with confidence using the crack measuring systems employed in the Canadian experimental program [1].

A study of the literature, [7] - [9], describing extensive experimental work carried out in Europe on similar steels, was performed to obtain realistic values of material growth rate constants. The values of C and m, chosen for these studies were:

$$m = 3.0$$
$$C = 5.36 \times 10^{-12}$$

and the units in equation (1) were m/c for da/dN and MPa $m^{\frac{1}{2}}$ for ΔK.

An extensive series of computer calculations were carried out on five specimen thicknesses at five stress levels of 75, 100 150, 200, and 300 MPa and a stress ratio of 0.05 for different initial crack depths to assess the behaviour of the prediction program. An example of the growth prediction behaviour of a/N for the three fracture mechanics models considered, compared with experimental results is shown in figure 8.

Figure 9 shows a S-N plot of the predicted propagation life, using an initial crack size of 0.5 mm, for the stress ranges and plate thicknesses investigated in the Canadian experimental program compared with experimental results. This figure clearly demonstrates the so called thickness effect, i.e., the reduction in fatigue life with increasing section thickness, and the good correlation between predicted and experimental results.

The predicted results produced in this work were also compared, on life - thickness plots, with experimental results from research centres involved in the European Coal and Steel, (ECSC), research program. These results were obtained from references [10] - [12] and are shown in figures 10, 11 and 12 for stress ranges of 100, 150 and 200 MPa. The points shown on these plots represent the total life of the plate joints, therefore the predicted results were modified to

include an initiation period. This initiation period was chosen to be 30% of the propagation life, a value arrived at after study of the Canadian experimental results shown in figure 2.

These plots further demonstrate the thickness effect and show the life predictions as a function of thickness for the three fracture mechanics models considered. It can also be seen from these plots that as the thickness of the specimen and the stress level increases the MC case tends towards the SFC case.

The predicted results for the present work are also presented on a log-log plot of relative fatigue strength at $1x10^6$ cycles versus thickness in the same manner as Gurney [5] and the latest edition of the Department of Energy Guidance Notes [13]. Shown on this plot, figure 13, is the Gurney line of slope -0.25 together with the predicted line with a slope of -0.3. Also plotted are the experimental results from the Canadian [1], the European [11], the British Steel Corporation [10] and UKOSRP [11] programs for an endurance life of $1x10^6$ cycles and normalised for a thickness of 32 mm.

The data shown in this plot includes results of specimens tested in the as welded condition, those subjected to PWHT, those welds tested in the load-carrying and non-load-carrying conditions and also those tested at various R ratios. It can be seen from this data and similar plots given elsewhere in the literature that the available results would seem to support the suggestion that the thickness effect shown would be better described by a line of slope greater than -0.25.

6. CONCLUSIONS

A fracture mechanics fatigue crack growth model for welded "T" plate joints has been reported. This model attempts to account for multiple initiation and crack coalescence in the predicted life of the joints for a wide range of thickness and stress range.

Stress intensity relationships were developed for straight-fronted and semi-elliptical weld toe cracks using the finite element method and the resulting predictions for SFC, SC and MC cases are reported.

The predicted results using the MC fracture mechanics model are in good agreement with and show similar trends to the observed experimental data.

7. ACKNOWLEDGEMENT

This research was funded by the Physical Metallurgy Research Laboratories of the Canada Centre for Minerals and Energy Technology.

8. REFERENCES

[1] Mohaupt, U.H., Burns, D.J., Vosikovsky, O., Bell, R., and Kalbfleisch, J.D.: "Fatigue Crack Development and Thickness Effects in Welded Plate to Plate Connections", Intl. Offshore Conf., Steel in Marine Structures, Paper TS3, Delft, June 1987.

[2] Barsoum, R.S.: "On the Use of Isoparametric Finite Elements in Linear Fracture Mechanics", Intl. J. of Num. Methods in Engineering, 10-1, 1976.

[3] Bell, R.: "Determination of Stress Intensity Factors for Weld Toe Defects" Carleton University Contract Report, DSS File No. 22ST.23440-2-9083/1, Oct. 1985.

[4] Newman, J.C. and Raju, I.S.: "An Empirical Stress Intensity Factor Equation For the Surface Crack", Engineering Fracture Mechanics, Vol. 15, No. 1-2, pp. 1985-192, 1981.

[5] Gurney, T.R.: "The Effect of Thickness on the Fatigue Strength of Welded Joints", Second Intl. Conf. on the Behaviour of Offshore Structures, London, 1979.

[6] Vosikovsky, O., Bell, R., Burns, D.J. and Mohaupt, U.H." "Fracture Mechanics Assessment of Fatigue Life of Welded Plate T-Joints, Including Thickness Effects", Proceeding of 4th Intl. Conf. on Behaviour of Offshore Structures (BOSS '85), pp. 453-464, Delft, 1985.

[7] Thorpe, T.W., Scott, P.M., Rance, A., and Silvester, D.: "Corrosion-fatigue of BS4360:50D Structural Steel in Seawater", Report AERE Harwell -R 10679, November 1982.

[8] Berge, S.: "Effect of Plate Thickness in Fatigue Design of Welded Structures" Offshore Technology Conference, Paper 4829, Houston, May 1984.

[9] Smith, T.J., and Hurworth, S.J.: "The Effect of Geometry Changes upon the Predicted Fatigue Strength of Welded Joints", Welding Institute Report No. 224/1984.

[10] Webster, S.E., Augsten, I.M. and Rudd, W.J.: "Fatigue, Corrosion Fatigue and

Stress Corrosion of Steels for Offshore Structures", British Steel Corp., Report FR103-6/832, April 1982.

[11] Long, D. and Webster, S.E.: "United Kingdom Offshore Steels Research Project", UKOSRP-II/PSC/P86-4, Feb. 1986.

[12] deBack, J. and Vaessen, G.H.G.: "Effect of Plate Thickness, Temperature and Weld Toe Profile on the Fatigue and Corrosion Fatigue Behaviour of Welded Offshore Structures", Report F7.4/81, Delft Institute of Technology, May 1984.

[13] UK Department of Energy,: "Offshore Installations: Guidance on Design and Construction", HMSO, 1984.

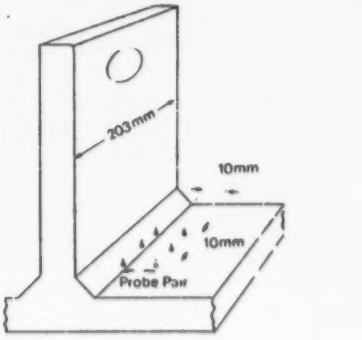

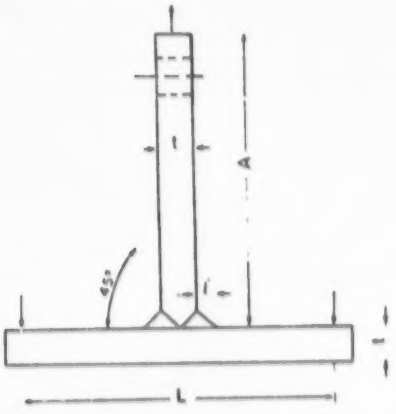

JOINT	t (mm)	l (mm)	L (mm)	A (mm)
A	16	8-12	300	406
B	26	14-18	442	406
C	52	26-30	442	406
D	78	38-42	584	457
E	103	52-56	726	457

Figure 1

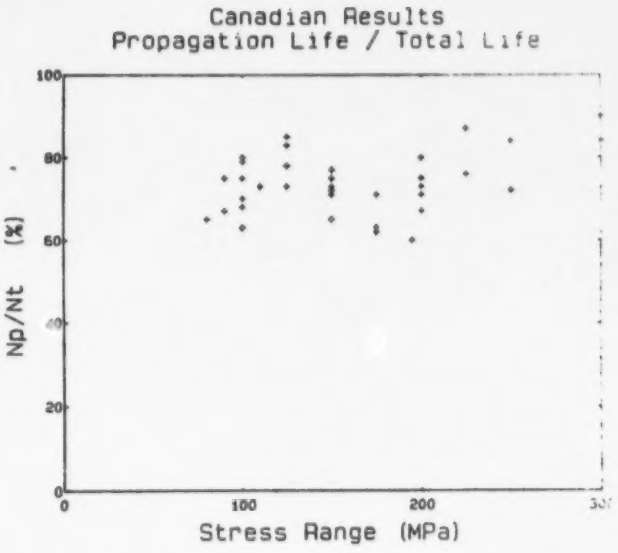

Figure 2

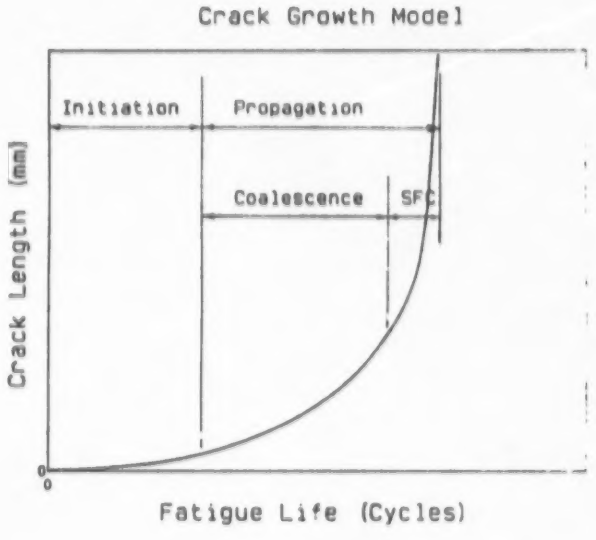

Figure 3

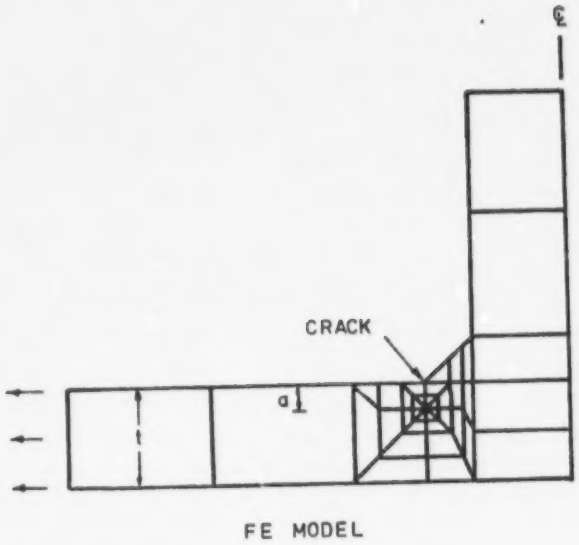

Figure 4

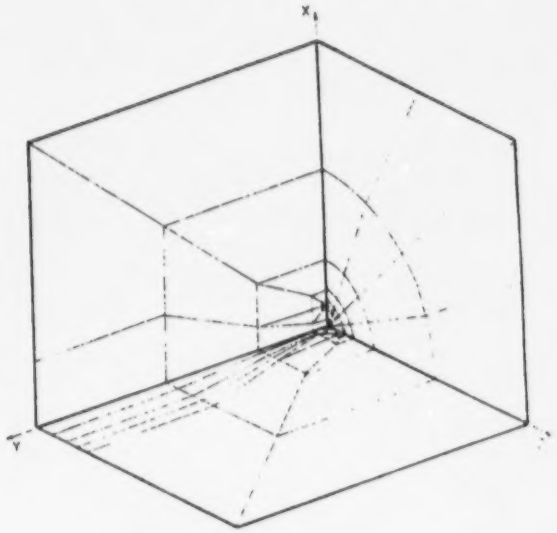

Figure 5(a)

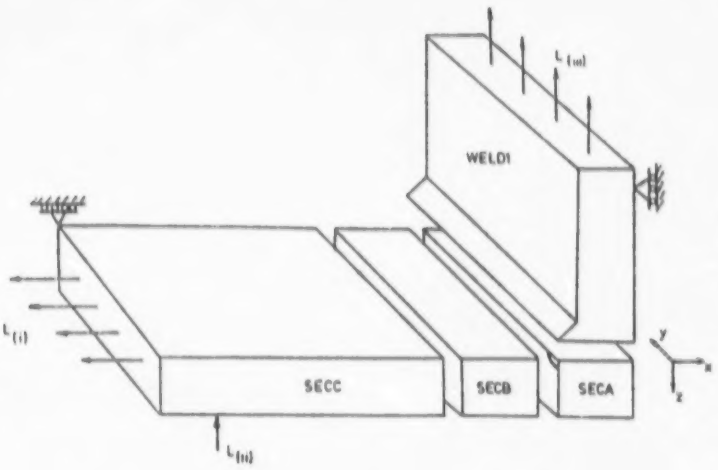

Figure 5(b)

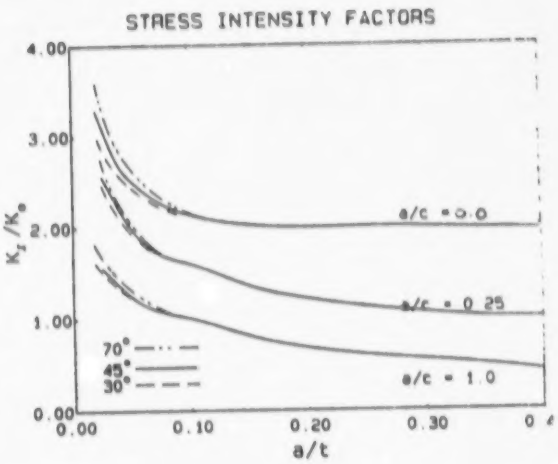

Figure 6

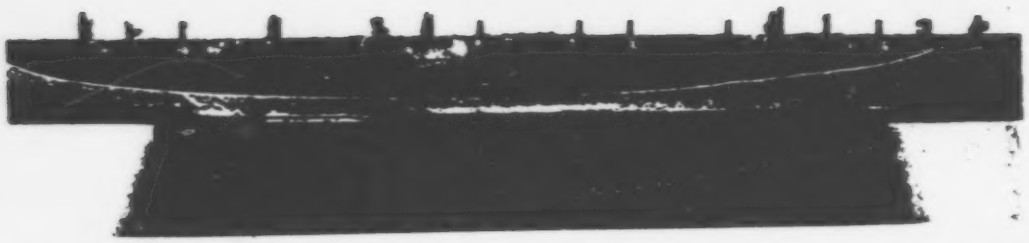

(a) t = 16 mm: $\Delta\sigma$ = 150 MPa

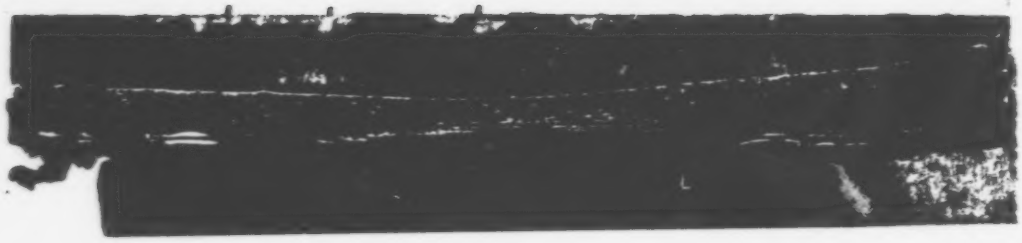

(b) t = 26 mm: $\Delta\sigma$ = 100 MPa

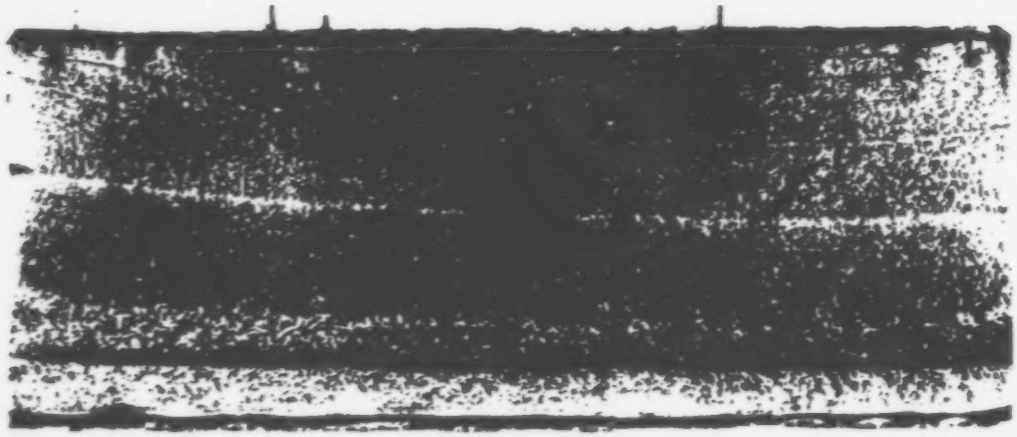

(c) t = 78 mm: $\Delta\sigma$ = 200 MPa

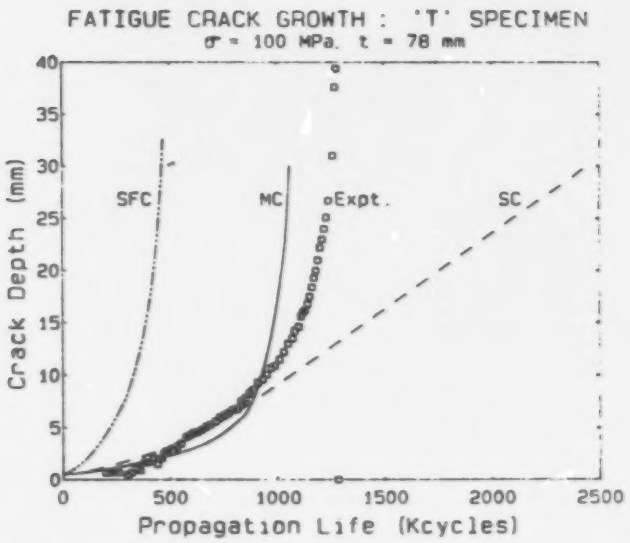

Figure 8

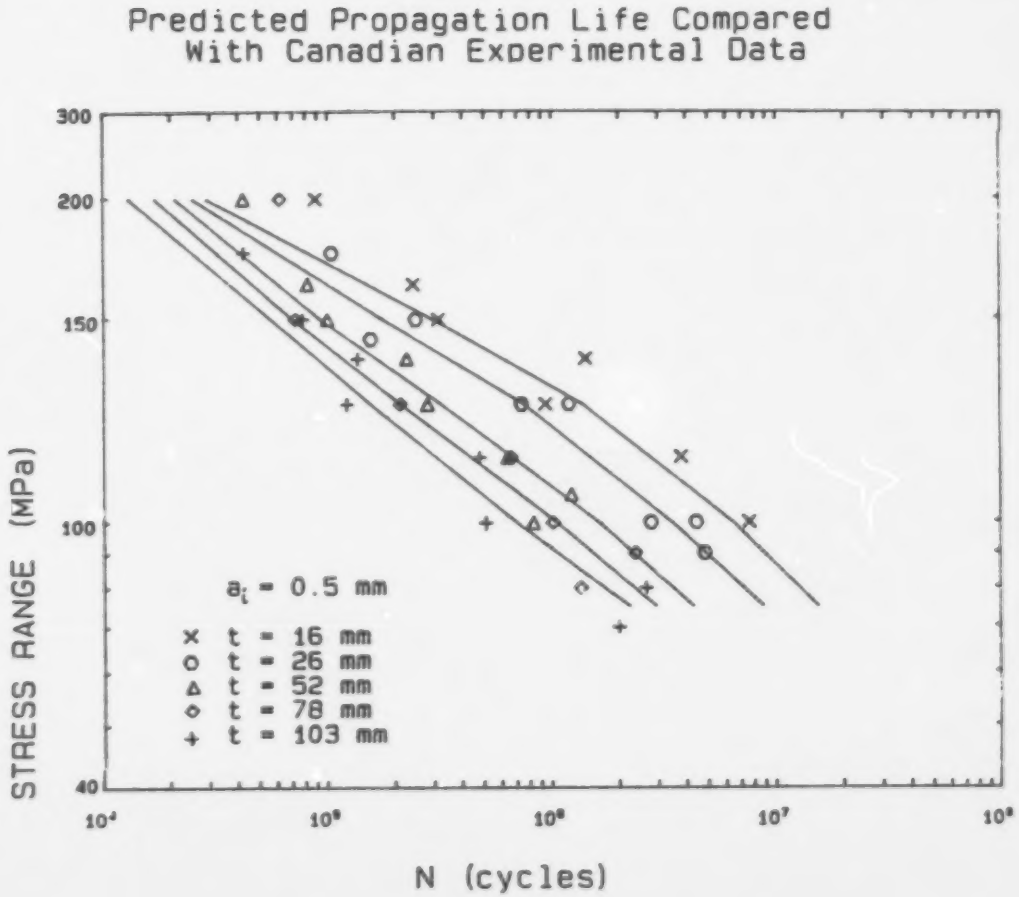

Figure 9

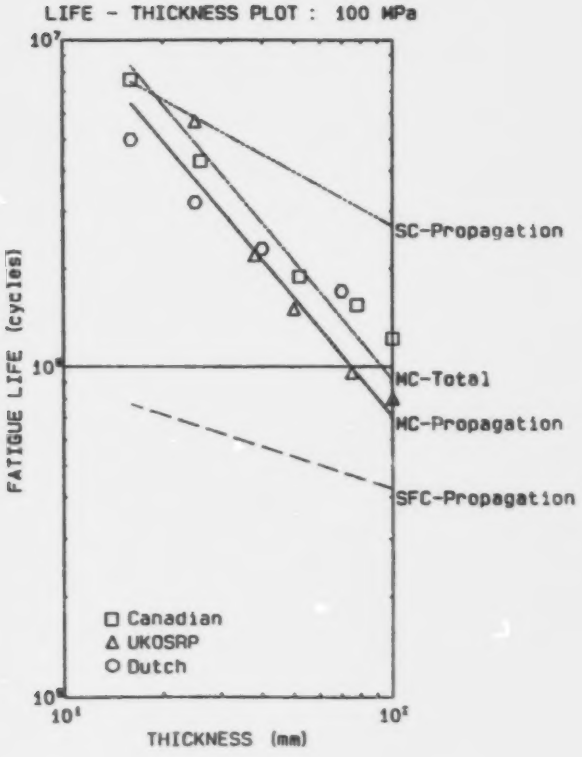

Figure 10

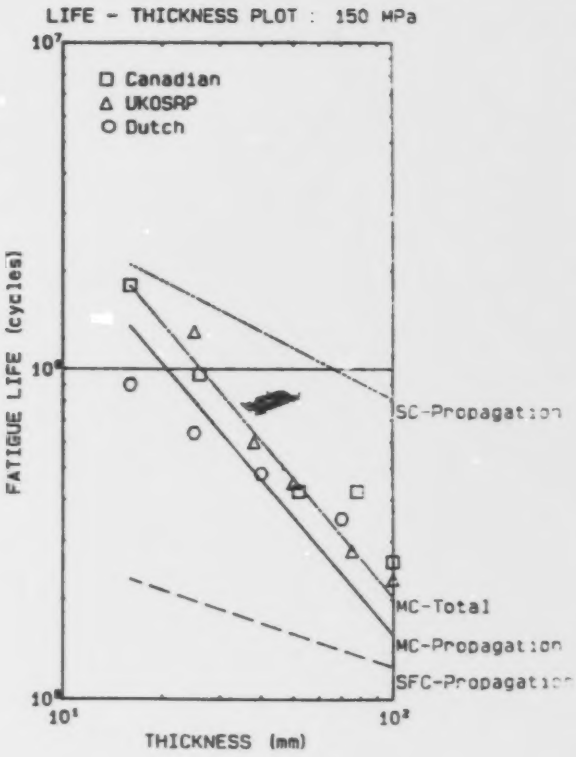

Figure 11

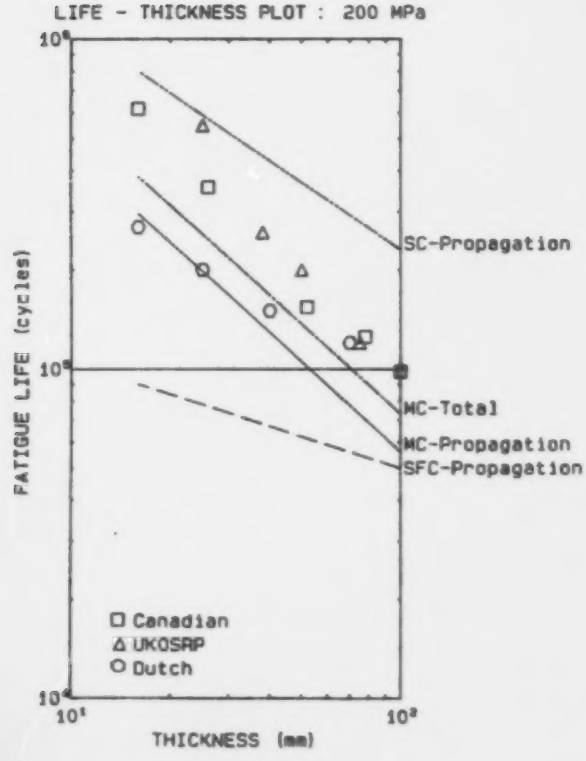

Figure 12

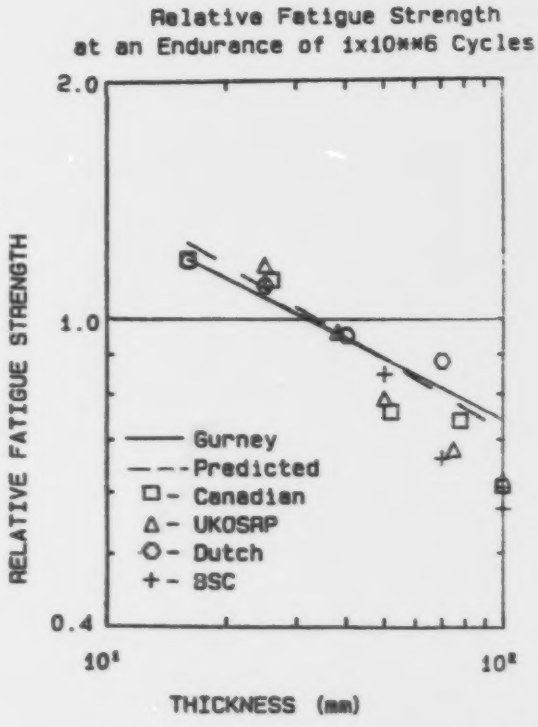

Figure 13

APPENDIX III

Dr. W. Tyson,
P.M.R.L
568 Booth Street,
Ottawa, Ontario.
K1A OG1.

May 02, 1986.

Re: IPC meeting for Delft Conference in 1987.

Dear Bill,

I attended the International Planning Committee for the International Offshore Conference on Steels in Marine Structures (Delft 1987) in Riso, Copenhagen on April 24, 1986.

My overall feeling of the planning meeting was favourable and I was given the impression the Canadian Offshore program is accepted on the same basis as the other European programs as making a valuable contribution to the body of knowledge on the behaviour of steels in marine structures.

The highlights of the meeting were as follows:

1. CANMET will be asked to give an overview of the Canadian Offshore Research Program. This will be at the beginning of the conference together with the ECSC, UKOSRP, and Norwegian programs. The presentation should be 10 - 15 minutes long.

2. There were 69 abstracts submitted and 51 were accepted.

3. The four Canadian abstracts were accepted as submitted.

4. Professor David Burns of Waterloo Univ. will be asked to present a plenary session lecture on Fatigue Crack Growth and Life Prediction.

In conclusion, from a Canadian point of view, the Canadian presentations to the Working Group II were extremely well received and the planning meeting was very favourable. I will give you further details of the plans for the conference when I meet you in the near future.

Yours sincerely,

Robert Bell,
Associate Professor.